

**Detection of Molecular Biomarkers involved in the Induction of EMT, migration and invasion, and drug resistance in breast cancer cells in 3D confinement**

By

Tamara N. Hill

Doctoral Dissertation Defense

Department of Bioengineering

The University of Texas at Arlington

Faculty Advisor: Dr. Young-tae Kim, Ph.D.

Date of Presentation: December, 2018

# Table of Contents

<b>CHAPTER 1: INTRODUCTION .....</b>	<b>1</b>
<b>1.1 METASTATIC BREAST CANCER .....</b>	<b>1</b>
<i>1.1.1 Statistics .....</i>	<i>1</i>
<i>1.1.2 Triple negative breast cancer (TNBC) .....</i>	<i>1</i>
<i>1.1.3 Therapeutic approaches and current challenges .....</i>	<i>5</i>
<b>1.2 MICROFLUIDIC SYSTEMS.....</b>	<b>9</b>
<i>1.2.1 Microfluidic systems .....</i>	<i>9</i>
<i>1.2.2 PDMS .....</i>	<i>9</i>
<b>1.3 OVERVIEW OF RESEARCH PROJECT .....</b>	<b>10</b>
<i>1.3.1 Significance .....</i>	<i>10</i>
<i>1.3.2 Objectives .....</i>	<i>10</i>
<i>1.3.3 Specific Aims.....</i>	<i>10</i>
<b>CHAPTER 2: DETECTION OF MOLECULAR MARKERS WHICH STIMULATE EMT AND MIGRATION IN BREAST CANCER CELLS .....</b>	<b>12</b>
<b>2.1 INTRODUCTION .....</b>	<b>12</b>
<b>2.2 MATERIALS AND METHODS.....</b>	<b>13</b>
<i>2.2.1 Model for microfluidic microchannel device .....</i>	<i>13</i>
<b>2.2.2 MANUFACTURE OF PDMS MICROFLUIDIC MICROCHANNEL DEVICES .....</b>	<b>14</b>
<b>2.2.3 CELL LINE AND CULTURE .....</b>	<b>15</b>
<b>2.2.4 RECOVERY OF VIABLE MIGRATING MDA-MB-231 CELLS .....</b>	<b>16</b>

<b>2.2.5 PREPARATION OF WHOLE-CELL SAMPLES .....</b>	<b>16</b>
<b><i>2.2.6 Preparation of soluble protein fractions .....</i></b>	<b>16</b>
<b><i>2.2.7 Statistical Analysis .....</i></b>	<b>17</b>
<b>2.3 RESULTS .....</b>	<b>17</b>
<b><i>2.3.1 Viable migrating cell recovery from PDMS device.....</i></b>	<b>17</b>
<b><i>2.3.2 Grouping of migrating from non-migrating cells.....</i></b>	<b>17</b>
<b><i>2.3.3 Western Blot analysis of EMT-related proteins.....</i></b>	<b>18</b>
<b>2.4 DISCUSSION .....</b>	<b>21</b>
<b><i>2.4.1 Induction of increased EMT stimulating proteins in breast cancer cells .....</i></b>	<b>21</b>
<b>2.5 SUMMARY AND FUTURE STUDIES.....</b>	<b>24</b>
<b>CHAPTER 3: FABRICATION OF AN ENGINEERED BASAL LAMINA EQUIVALENT FOR CANCER CELL RESEARCH.....</b>	<b>25</b>
<b>3.1. INTRODUCTION .....</b>	<b>25</b>
.....	28
.....	29
<b>3.2 METHODS .....</b>	<b>30</b>
<b><i>3.2.1 Fabrication of the Engineered Basal Lamina Equivalent (EBL) .....</i></b>	<b>30</b>
<b><i>3.2.2 Material Characterization of EBL .....</i></b>	<b>30</b>
<b><i>3.2.3 Cell Cultures .....</i></b>	<b>31</b>
<b><i>3.2.4 Breast cancer Cell Culture on EBL .....</i></b>	<b>31</b>
<b><i>3.2.5 Quantification of Cancer Cell Protein Expression by Western Blot.....</i></b>	<b>32</b>
<b><i>3.2.6 Viability Analysis .....</i></b>	<b>32</b>
<b>3.3 RESULTS .....</b>	<b>33</b>
<b><i>3.3.1 Characterization of EBL .....</i></b>	<b>33</b>

3.3.2 Robust growth of different cell types on EBL .....	34
3.3.3 Western blot analysis of protein expression in breast cancer cells culture on EBL.....	35
3.3.4 Western blot analysis of protein expression in non-small cell lung cancer (NSCLC) cells culture on EBL .....	36
3.3.5 Drug response of breast and lung cancer cells after chemotherapy .....	40
3.4 DISCUSSION .....	42
 <b>CHAPTER 4: IDENTIFICATION OF CANCER STEM CELL MARKERS IN CELL POPULATIONS AFTER MIGRATION .....</b>	
<b>4.1 INTRODUCTION .....</b>	<b>46</b>
<b>4.2 MATERIALS AND METHODS.....</b>	<b>48</b>
4.2.1 Fabrication of device .....	48
4.2.2 Cell culture.....	48
4.2.3 Cell harvesting for western blot.....	49
4.2.4 Western blot .....	49
4.2.5 Drug pumping.....	50
4.2.6 Cell viability after drug treatment .....	50
4.2.7 Migrated cells re-seeded .....	50
<b>4.3 RESULTS .....</b>	<b>51</b>
4.3.1 CSC related biomarkers expression by migrated cells.....	51
4.3.2 Immunostaining of CSC and EMT markers.....	52
4.3.3 Highly regulated chemotherapy resistance for migrating cells expressing membrane drug efflux pumps .....	55
<b>4.4 DISCUSSION .....</b>	<b>62</b>
4.4.1 Stem cell markers.....	62

<i>4.4.2 Dox viability and drug pumping</i> .....	63
<i>4.4.3 Hypoxia</i> .....	64



## **Abstract**

Standard-of-care regimes for cancer treatment have become more effective and sophisticated over the last decade due to research developments which facilitate specific targeting of treatments to certain cancers, and the ability to provide specialized care to cancer patients. However, cancer treatments overall still fall short of preventing spread of disease from the primary tumor to secondary sites where they settle and form new more aggressive tumors. It is this stage of disease progression which results in the majority of cancer deaths. The long-term goal of this research is to develop a system for the effective high throughput screening of chemotherapeutic drugs (and possibly in combination with radiation therapy) that target migrating cancer cells, for metastatic cancer treatment. In Aim 1 we developed a polydimethylsiloxane (PDMS) microfluidic device equipped with microchannels for the study of proteome expression changes that are likely induced through Epithelial-to-mesenchymal (EMT) transition, a result of migration through confined three-dimensional (3D) space. Quantification of protein expression differences between cells that migrated, and cells that grew in a classical two-dimensional (2D) environment revealed a pattern of molecular changes associated with EMT which highly invasive MDA-MB-231 breast cancer cells likely underwent while migrating through the microchannels. While examining these differences between cells in the two different conditions, we were inspired to develop an Engineered Basal Lamina (EBL) for 2D culture of breast and lung cancer cells. Coating of cell culture well plates with the EBL revealed a significant difference in both protein expression and chemotherapeutic response from cells grown on the classic polystyrene coating. We further sought to examine in Aim 3, the induction of dedifferentiation of breast cancer cells upon migration through confined space, and the molecular properties associated with this process that render these cells completely unresponsive to Doxorubicin (DOX), a potent breast cancer drug whose mode of action is DNA intercalation and inhibition of macromolecular biosynthesis. We sought to uncover the genetic and epigenetic activities of the cancer cells upon collection from the microchannels and re-culture in a 2D

environment, as well as changes associated with multiple and extended migration events. This would likely uncover possible therapeutic targets for cells which have migrated to secondary sites.



# CHAPTER 1: INTRODUCTION

## 1.1 Metastatic Breast Cancer

### 1.1.1 Statistics

Breast cancer comprises one of the largest cancer groups in the United States and its metastasis leads to more deaths than many other diseases.(1) Excluding skin cancers, breast cancer is the most common cancer diagnosed among women in the United States, accounting for nearly 1 in 3 cancers.(2) A woman living in the United States has a 12.3%, or a 1-in-8, lifetime risk of being diagnosed with breast cancer. There were an estimated 1,685,210 new cancer cases reported in 2016, and 595,690 cancer deaths. Based on growth and aging of the U.S.(3) population, medical expenditures for cancer in the year 2020 are projected to reach at least \$158 billion — an increase of 27 percent since the year 2010, according to a National Institutes of Health analysis.(4) The development of efficient tools to use for the early detection and diagnosis, and effective treatment of cancer is an urgent and critical priority for healthcare.

### 1.1.2 Triple negative breast cancer (TNBC)

In contrast to many other cancers, TNBC cells are characterized by a lack of expression of the genes for estrogen receptor (ER), progesterone receptor (PR), and human epidermal growth factor receptor 2 (HER2) amplification.(5) It is an aggressive form of cancer with poor prognosis and limited treatment options as a result, because standard treatments for breast cancer consist of hormone treatments targeted to one of the three receptors. It is likely that fundamental molecular targets include pathways with multiple redundancies and pathway crosstalk, yielding mechanisms of compensation for cells against apoptosis. If only one molecular pathway is selectively inhibited, the efficacy of the therapeutic strategy would likely be

undermined by a compensatory pathway.(5) Understanding the molecular basis of TNBC is therefore crucial for effective new drug development.

TNBC is a heterogenous disease which renders it significantly more difficult to treat than most cancers.(6) TNBC tumors of the “claudin-low” subtype have particularly poorer prognosis than hormone-positive tumors. This is due to the low expression of mRNA for claudins 3, 4, and 7 which are components of the tight junctions between epithelial cells joining neighboring cells and thereby restricting epithelial transport via the paracellular pathway. These junctions maintain polarity of epithelial cells by reducing the diffusion of membrane proteins between apical and basal surfaces. In addition, basal-like breast cancers account for 47% - 88% of all TNBC.(7) Burstein et al. identified, by DNA and RNA genomic profiling, six stable TNBC subgroups with distinct clinical outcomes defined by specific overexpressed or amplified genes.(8) They also identified specific molecules that define each subgroup, serving as subgroup-specific biomarkers as well as potential targets for treatment of these aggressive breast cancers. Table 1. outlines the six molecular subtypes which make TNBC a heterogenous disease to treat and implications for a need for combination therapy.

### **1.1.2.1 Metastatic TNBC**

Less than 30% of women with metastatic breast cancer survive five years and virtually all women with metastatic TNBC will ultimately die of their disease despite systemic therapy.(9–11) Breast carcinomas with particular patterns of differentiation or gene expression have characteristic sites to which they metastasize. For example, the bone is a common site of first metastasis in women with hormone receptor positive carcinomas.(12) In an attempt to uncover the pattern of metastatic spread for TNBC, *Dent et al.* demonstrated that women with TNBC were four times more likely to experience a visceral metastasis (metastases of internal organs including liver, lung, and body cavities) within five years of diagnosis.(10) They also reported deaths occurred within 10 years after initial diagnosis vs. 18 years for ER-receptor

positive cancer patients. Furthermore, that time from distant recurrence to death was much shorter for TNBC patients.

Factors influencing the development of breast cancer metastases largely include tumor size, histologic grade, lymphovascular spread, nodal involvement, and receptor status. It has long been accepted that, like many other tumor types, breast cancer spread demonstrates a nonrandom, organotropic metastatic pattern, a theory known as the “seed and soil” hypothesis first popularized by Paget in 1889(13–15), Figure 1.1. The organ-specific metastatic cells found to be preexistent in the parental cells were able to be enriched in vivo in their target organs, as first documented in experimental metastasis assays in the 1970s. In the “seed and soil” hypothesis, tumor metastasis is explained by primary tumors preparing the local microenvironment of distant organs for tumor cell colonization even before their arrival. The pro-metastatic tumor cells (the “seed”) colonize in specific organ sites (the “soil”) where the microenvironment is favorable for metastasis.(16)

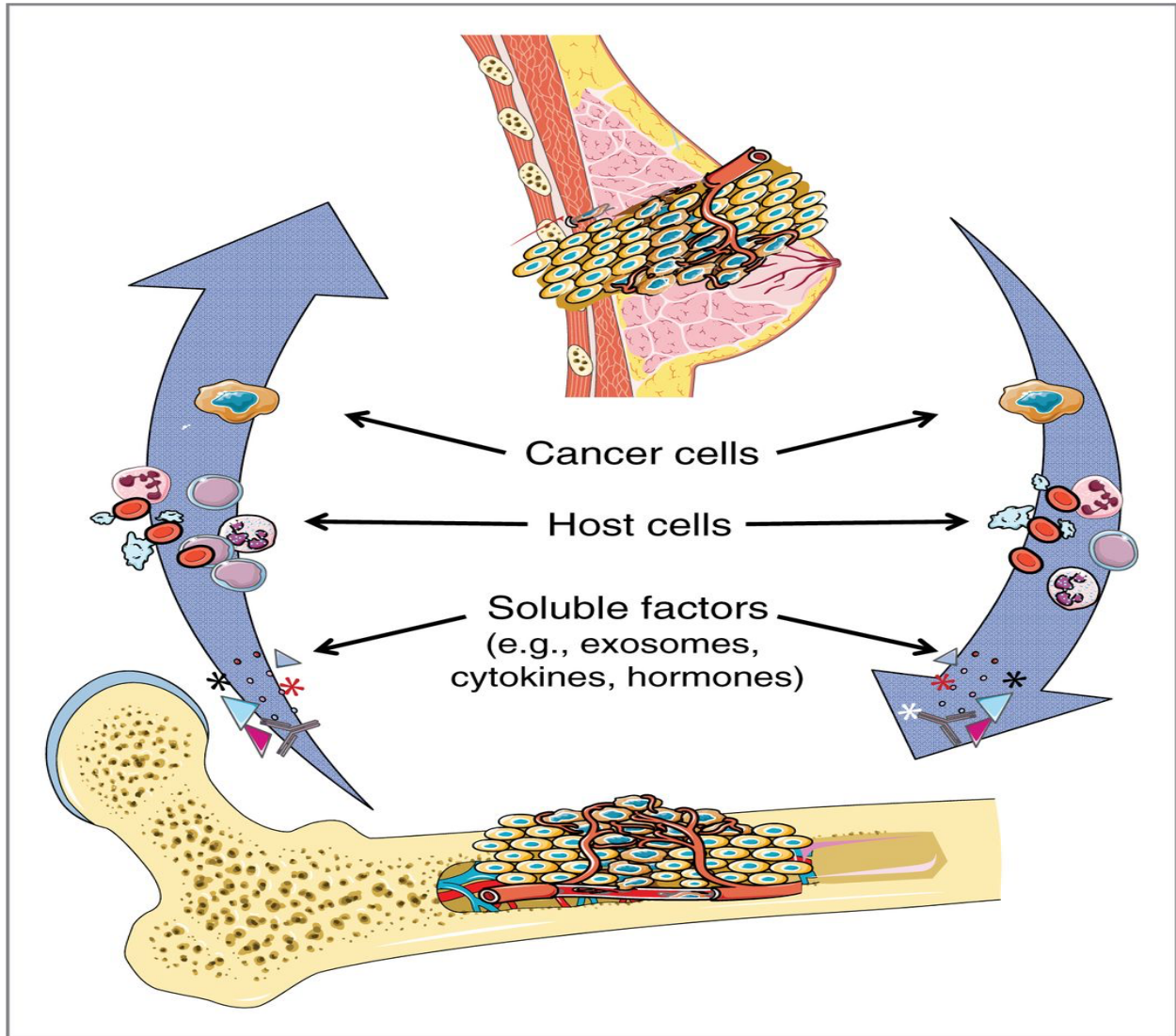


**Figure 1.1** Summary of tumor cell responses to chemokine signaling involved in the “Seed and Soil” conditioning of metastatic sites in breast cancer.(16)

### 1.1.2.2 Molecular pathogenesis

A major role played in the transformation of tumor cells to invasive metastatic cell is that of EMT. EMT is a process characterized by the loss of cellular polarity and cell to cell adhesion in epithelial cells. These morphological changes activate migratory properties in the cells, inducing a mesenchymal stem cell phenotype.(17) The mesenchymal properties of these cells makes this process essential during embryonic

development and wound healing. During embryonic development, cells can transition between epithelial and mesenchymal states in a highly plastic and dynamic manner. A shift toward the mesenchymal state (EMT) modifies the adhesion molecules expressed by the cells, allowing them to adopt a migratory and invasive behavior. The reverse of this process, mesenchymal to epithelial transition (MET), is associated with a loss of this migratory freedom, with cells adopting an apico-basal polarization and expressing the junctional complexes that are hallmarks of epithelial tissues.

An active role of EMT during metastasis is suggested by the finding that the gain of expression of mesenchymal markers in circulating tumor cells of patients with breast cancer predicts poor prognosis more accurately than only considering epithelial cytokeratin markers.(18) Several key signaling pathways contribute to this process, namely TGF- $\beta$  and Wnt, known inducers of EMT and promoters of dedifferentiation. *Abram BK et al.* found that the majority of disseminated tumor cells detected in the bone marrow of breast cancer patients with a CD44<sup>+</sup>/CD24<sup>-</sup> correlated with a higher bone metastasis.(19) Countless studies have confirmed a major role of aldehyde dehydrogenase 1 (ALDH1), a detoxifying enzyme responsible for the oxidation of intracellular aldehydes, in breast cancer metastasis. *Atkas et al.* demonstrated that EMT markers; Twist1, Akt2, PI3Ka were increasingly expressed in circulating tumor cells as opposed to noncirculating tumor cells.(20) They also found that lower sensitivities to treatment were associated with these phenotypes.

### **1.1.3 Therapeutic approaches and current challenges**

As previously mentioned, the difficulty in effectively treating TNBC is represented by its genetic heterogeneity, as is characterized by the presence of six subtypes. The importance surrounding discovery of effective treatments for this disease is illustrated by its poor prognosis, high mortality in comparison to other cancers, and lack of effective specific targeted therapy available.

The therapeutic strategies for the management of TNBC are targeting DNA repair complexes like (platinum compounds and taxanes), p53 like (taxanes), cell proliferation like (anthracycline containing regimen) and targeted therapy.(21)

<b>TNBC Subtype</b>	<b>Molecular characterization</b>	<b>Treatment targeting options</b>	<b>Reference</b>
<b>BL1</b>	Elevated DNA damage response (ATR/BRCA) pathways	Genomic instability	(22,23)
<b>BL2</b>	Uniquely enriched in growth factor receptors such as: EGFR, MET, & EPHA2	Genomic instability	(24)
<b>IM</b>	High expression of STAT genes	Immune check-point inhibitors	(25)
<b>M</b>	Enriched in genes involved in: cell motility, extracellular receptor interaction, and cell differentiation	DNA-damaging agents	(26)
<b>MSL</b>	Enrichment of genes modulating growth factors: IP metabolism, EGFR, PDGF, calcium signaling, G-protein coupled receptor, ABCG2	DNA-damaging agents	(27)
<b>LAR</b>	ER-negative. However, heavily enriched in hormonally regulated pathways including steroid synthesis, porphyrin metabolism, & androgen/estrogen metabolism.	Anti-androgens	(11)

**Table 1.** Six subcategories of TNBC and representative variability in how to treat each subcategory.

The specific adjuvant regimens that may be most effective for TNBC are still to be determined. Numerous large randomized trials have established the benefit of adjuvant anthracyclines and taxanes in breast cancer.(8) All options are proposed in first-line treatment but the majority of recommendations indicated taxanes for first-line therapy while recommendations for second-line therapy were more commonly single agent capecitabine or combination of capecitabine and vinorelbine, or gemcitabine and vinorelbine or a platinum-based regimen.(28)

The most frequently recommended platinum-based regimens for first-line therapy and second-line is cisplatin plus gemcitabine, carboplatin plus paclitaxel and carboplatin plus gemcitabine.(29) Several targeted therapies are being successfully developed like Poly (ADP-ribose) polymerase-1 (PARP-1), which is a nuclear DNA-binding enzyme activated by DNA strand breaks and has a key role in the signaling of DNA single-strand breaks as part of the repair process. Lastly, iniparb has been shown improved patient response in combination with chemotherapy.(30) However, progression to phase II trials will be needed to yield more dependable results.

### **1.1.3.1 EMT-associated resistance to cancer therapeutics**

Cancer therapy is often associated with two major forms of drug resistance, a) de novo and b) acquired. Patients who are initially refractory to therapy (de-novo) show intrinsic drug resistance. Patients that initially respond to therapy typically relapse (acquired) as a consequence of drug resistance. A significant body of evidence suggests that reversible epigenetic changes that take place as a result of chemotherapy tumor treatment may be to the major cause of acquired resistance.(31) These reversible epigenetic changes are likely due to EMT reprogramming of cells.

In addition, some reports also suggest that basal, mesenchymal-like cancers are initially more sensitive to neoadjuvant chemotherapy than epithelial luminal tumors.(32) Yet, despite the initial responses, patients with basal cancers are given the worst prognoses, suggesting that these mesenchymal-like cancers are more prone to developing drug resistance.(33) It is possible that epithelial-like cancers are initially more sensitive to targeted therapies, such as EGFR and HER2 antagonists, whereas mesenchymal cancers are more sensitive to DNA damaging agents such as doxorubicin.(34)

While chemo- and radiotherapy treatments have yielded results that extend survival time in patients, it remains a mystery what mechanisms underlie resistance to these treatments, which prevents overall complete recovery at higher rates.(35,36) A large body of evidence suggests EMT as a major contributor

of evolved treatment resistance, and subsequent relapse.(37,38) The usual pattern of induction of cellular plasticity tends to involve decreased uptake of water-soluble drugs, various changes in cells that affect the capacity of cytotoxic drugs to kill cells, and increasing energy-dependent efflux of hydrophobic drugs that can easily enter the cells by diffusion.(39) In addition, transcription factor activity such as altered expression of drug-metabolizing enzymes and export pumps, and suppression of apoptotic pathways have been increasingly discovered to take pivotal roles in breast cancer treatment resistance.(40)

Energy-dependent drug efflux transporters have particularly been shown to play a crucial role in chemoresistance. In breast cancer, ATP-binding cassette (ABC) transporters including P-glycoprotein (P-gp or MDR1) and breast cancer resistance protein (BCRP) have been shown to not only be shown to reduce the concentration of drug inside the cell, these upregulated receptors have also demonstrated involvement in the reprogramming of metastatic breast cancer cells.(41) Growth factors have also shown transcription activity during invasion and metastasis.(26,42) In breast cancer; tumor necrosis factor (TNF- $\alpha$ ), transforming growth factor (TGF- $\beta$ ), epithelial growth factor (EGF), fibroblast growth factor (FGF), insulin growth factor (IGF), and platelet derived growth factor (PDGF) and various other extracellular stimuli have shown increased expression during invasion of cancer cells.(43) One study found that cis-platinum treatment of highly invasive breast cancer cells increased TGF- $\beta$  mRNA levels and the secretion of active TGF- $\beta$ , which enhanced growth arrest that facilitated repair of damage, thus rendering these cells resistant to cis-platinum killing.(33) Increased IGF-1 levels were reported to stimulate metalloproteinase (MMP) secretion through induction pathways, leading to ECM degradation by MMPs and rescue of breast cancer cells from chemotherapy-induced cell death.(44) Highly invasive breast cancer cells have shown elevated levels of transcription factor, Twist, which upregulates the transcription of Akt-2 to promote cell survival and resistance to paclitaxel.(45) Slug and Twist transcription factors have been reported to closely correlate with poor prognosis in breast cancer patients. *Jeong et al.* mentioned that EMT was significantly related to high histological grade triple-negative phenotype but not predictive of disease-free survival in



breast cancer.(39)

In short, inhibition of EMT either by strategic targeting of proteins or genes may prove critical in the fight against breast cancer treatment resistance. Some authors have shown promising results by specifically reversing EMT, transforming these invasive cells back to an epithelial phenotype with stable physiologically stable expression of proteins that promote cell-cell contact and epithelial markers.

## **1.2 Microfluidic systems**

### **1.2.1 Microfluidic systems**

Microfluidics comprise methods and designs which involve volumes in microchannels of 1  $\mu\text{m}$  and above, laminar flow fluids, and controlled molecular concentrations.(46) The method has become most useful for its ability manipulate fluids and reagents within miniaturized platforms. Materials used have become more sophisticated, progressing from silicone and glass to polymers that are much more flexible and economical.(47) Advantages to using microfluidic devices experimentally in cancer research are a need for reduced sample size and reagent consumption, short processing times, enhanced sensitivity, and real-time analysis. Research applications have developed into single cell assays for disease diagnosis, manipulating RNA, researching cancer progression in non-conventional ways.

### **1.2.2 PDMS**

Polydimethylsiloxane (PDMS) is the common polymer used in fabricating microfluidic system. There are two chemical components required for fabrication of solid PDMS, silicon elastomer and cross-linker or curing agent. At room temperature, each of these chemicals maintain in liquid. Once mixed, they eventually form solid by crosslinking. Being an organic polymer that with flow properties, hydrophobic, non-toxic, inert, and clear makes is particularly useful in for studying cellular activities in a liquid medium. Similar to its usefulness in fabrication of contact lenses, the clear material provides a facile method for screening cellular migration and activity in real-time.(48)

## **1.3 Overview of Research Project**

### **1.3.1 Significance**

To date, TNBC has remained one of the most invasive cancers, characterized by poor prognosis and unavailable effective treatment. Molecular transcription targets and downstream events are being widely investigated, with the intent of pinpointing genome-wide biomarkers which will make specific disease targeting an effective tool to treat and eliminate metastasis and disease progression. Discovery of such biomarkers would be a significant step forward in the maintenance of breast cancer and yield increased disease-free survival clinically.

### **1.3.2 Objectives**

The short term objectives of this study are investigate relevant biomarkers for the reversal of EMT, and thus molecular inhibition of motility, reprogramming, and invasiveness of TNBC cells. Locating effective targets which stimulate multiple downstream cascades inducing EMT may provide effective tools to switch migratory cells back to and mesenchymal-to-epithelial (MET) phenotype, suppression the gene silencing/activation involved in invasive cellular programming. Long term objectives of this study involve clinical analysis of target genes and proteins, along with adjuvant therapy, in the design of molecular inhibitors and novel drugs which will effectively target and treat the disease with clinical significance.

### **1.3.3 Specific Aims**

**Aim 1: Detection of Molecular Markers Which Stimulate EMT and Migration in Breast Cancer Cells**

A novel PDMS microfluidic device was outfitted with microchannels to aid in migration of breast cancer cells and subsequent quantification of protein expression changes which take place during the process of migration.

### **Aim 2: Fabrication of an Engineered Basal Lamina Equivalent for Cancer Cell Research**

A basal lamina film was fabricated for the culture of breast and lung cancer cells. This film was used to detect native protein expressions among cancer cells as they migrate across and prepare to degrade the underlying basement membrane. This cell culture model was also used as a drug screening tool to correlate possible protein expression changes with induced drug resistance.

### **Aim 3: Contribution of subpopulation of reprogrammed tumor cells to disease progression**

A novel microfluidic device containing a seeding chamber and reservoir was used to detect protein expression of target proteins in different subcellular locations at different stages of migration. Drug screening was also quantified at different stages of migration, uncovering the highly resistant and invasive nature of this subpopulation of migrating cancer cells.

#### **1.4.4 Innovative Aspects**

Novel aspects of this research include the ability to efficiently compartmentalize cancer cells in different conditions, retrieve them in high yields, and study intracellular changes which take place in response to changes in their microenvironment. The ability to the same cell line in 2D monolayer completely separate from cells migrating in confined 3D space facilitates real-time culture and collection of these cells quickly and without the need for separate protocols. The presence of microchannels within the device eliminates the need to genetically alter the cells or use non-3D means such as scratch-assays, to study different mechanisms employed by the cells during this activity. Finally, the ability to screen cellular responses to drugs before, during, and after cells have migrated provides a more accurate and real-time depiction of

cancer activity as more invasive cells branch away from the tumor, and avoid cellular apoptosis as they relocate and settle to distant sites. These novel aspects taken together render this system a unique and efficient in vitro platform for the investigation of biomarkers which may lead to inhibitors or combination therapy regimes by which breast cancer therapy more targeted and effective.

## **CHAPTER 2: DETECTION OF MOLECULAR MARKERS WHICH STIMULATE EMT AND MIGRATION IN BREAST CANCER CELLS**

### **2.1 Introduction**

Treatment often includes chemotherapy, radiation, and tumor excision. However, the pitfalls that accompany these treatments include inability to efficiently target and destroy residual and migrating cells. Because these are the cells which are typically the cause of end stage mortality, they have been the target of many studies to determine molecular events which lead to their ability to dissociate from a primary tumor and invade the circulation and other tissues.(49) Many studies have utilized the petri dish, scratch assay and other inefficient forms of 2D environment to study migrating cancer cells. However, these methods neglect to stimulate molecular, genetic, proteomic, and cell surface changes the cells naturally undergo which enable migration to sites distant from the primary tumor. During migration, cells acquire the ability to squeeze through the 3D environments of blood and lymphatic capillaries 3-60  $\mu$ m in diameter. Migration through such a confinement of space has been reported to stimulate a change in cell surface activity needed to endow these cells with the capacity to function under circumstances quite different from those of cells in another 3D environment such as a tumor. EMT is a conversion process which stationary cells undergo to acquire motility.(50) This process is pivotal during embryonic development and wound healing. However, subsequent adaptation of this transition has supplied cancer cells with the capacity to become

migratory and invasive. These cells, through genetic signaling, take on a modified proteome which furnishes them with the ability to detach from a primary tumor, extravasate blood and lymph vessels, and settle forming colonies in distant tissues. The concern is that culture of cells under non-biomimetic conditions would fail to stimulate these migratory changes in cells.

We have designed a novel microchannel device made of polydimethyl siloxane (PDMS), which was able to stimulate the 3D microenvironmental conditions a malignant migrating cell travels, enabling molecular expression changes which we can detect, analyze, and possibly utilize in the design of clinical targets. This device facilitates 3D migration of MDA-MB-231, an aggressive line of breast cancer cells, and subsequent collection of these cells in substantial quantities. It has also provided a tool for the spatial differentiation between breast cancer cells grown in the 2D environment vs. those grown in the microchannels. Cells were seeded into 6-well plates and allowed 10 days to grow and migrate through microchannels. When a sufficient number of cells occupied microchannels, cells were collected and analyzed, demonstrating differences in protein expression as compared to cells cultured in a 2D environment. This novel device has provided for the detection and analysis of changes in the expression levels of proteins which impart to the cell the ability to undergo a transition from an epithelial to a mesenchymal phenotype.

## **2.2 Materials and methods**

### **2.2.1 Model for microfluidic microchannel device**

Using Autocad software and Solidworks, we were able to design a microchannel array that included a total of 600 microchannels placed parallel to each other (Fig. 2.2.1). Each microchannel had a cross sectional area of  $5 \times 12 \mu\text{m}$  (width x height) generating sufficient 3D physical confinement for cancer cell migration. The microchannel was intentionally made 5mm long to recruit more migrating cells and the distance between every two microchannels was  $30 \mu\text{m}$ . The whole array was approximately  $5 \times 21 \text{mm}$  (length x

width) which not only provided enough space to house numerous migrating cells but also allowed visualization for the user while doing cell collection process.

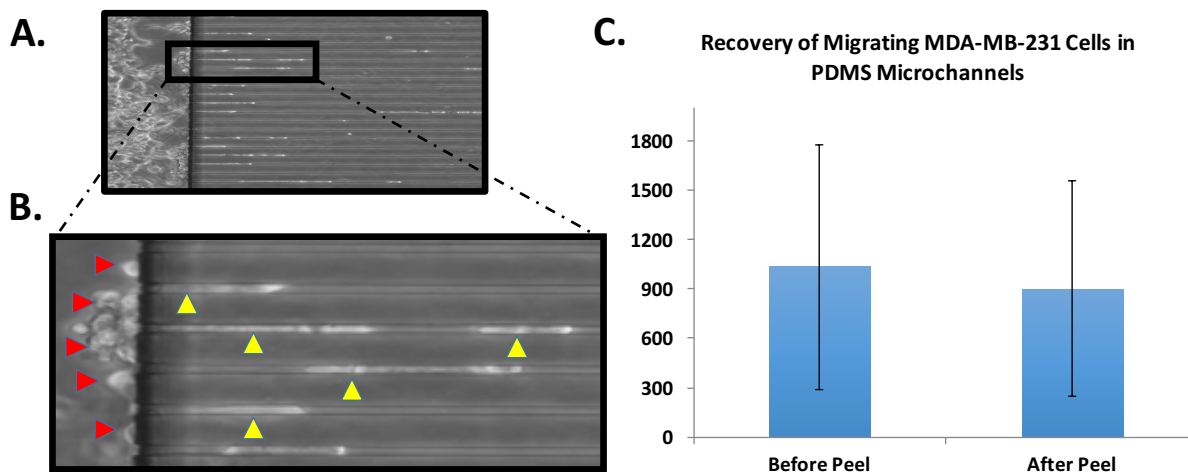


**Figure 2.2.1 Microchannel device for collecting migrating cells.** (A) Image of PDMS microfluidic device containing array of microchannels  $5 \mu\text{m}$  in width. (B) Inset magnification of device: red arrowheads, MDA-MB-231 cells grown in 2D; yellow arrowheads, MDA-MB-231 cells migrating through  $5 \mu\text{m}$  channels. (C) Quantification of cells in microchannels before and after peeling device from substrate.

### 2.2.2 Manufacture of PDMS microfluidic microchannel devices

The microfluidic devices were assembled by utilizing soft and standard photolithography. In order to construct microchannels with a  $12 \mu\text{m}$  height, an SU-8 photoresist (Microchem Corp, Newton, MA) was employed to photopattern a silicon wafer. Polydimethylsiloxane (PDMS) (Sylgard 184 Silicone Elastomer Base, Dow Corning) was cured with Sylgard 184 (Silicone Elastomer Curing Agent, Dow Corning) (10:1 ratio). The cured PDMS was then inserted onto the wafer, baked for 10 minutes ( $150^{\circ}\text{C}$ ) and peeled. Once peeled, The microchannels were opened by cutting across each channel's edges. As a result, the microchannels varied within 3 to 4mm in length. Devices were sterilized with 70% ethanol, then placed microchannel-side-down onto surface of wells in 6-well plate, Fig. 2.2.2A, G.

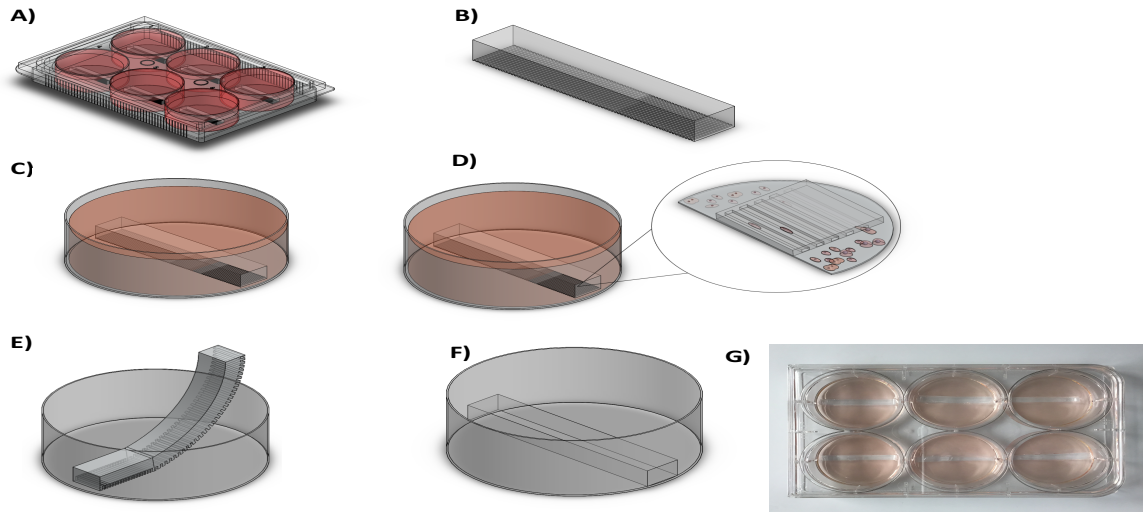


**Figure 2.2.2. Combined culture of 2D and migrating breast cancer cells.** (A-F) Schematic of cell culture procedure with microfluidic device. (A) Devices placed channels-side-down in 6-well plate. (B) Microfluidic device with microchannels. (C) Single well containing device. (D) Schematic of migrating cells vs. 2D cells, in culture. (E) Device being peeled from substrate for cell collection. (F) Single well containing device with no channels (control). (G) Image of 6-well plate contain culture with 5 devices with microchannels, and 1 device void of channels (control).

### 2.2.3 Cell line and culture

Cells were donated by University of Texas Southwestern. Human aggressive breast cancer cell lines MDA-MB-231, and non-aggressive breast cancer cell line MCF7 were both maintained in DMEM/F-12 medium supplemented with 10% fetal bovine serum. We set up each 6-well culture to have 5 devices with microchannels, and 1 device absent of microchannels as a control, Figure 2.2.2 F. All 6 wells were coated with collagen overnight and rinsed with PBS. Cells were cultured at  $100 \times 10^3$  cells/well and maintained up to 10 days to obtain the highest number of migrating cells.

#### **2.2.4 Recovery of viable migrating MDA-MB-231 Cells**

Cell migration was imaged by fluorescent microscopy. Cell nuclei were stained with Hoeschst<sup>®</sup> 33342 (Life Technologies) fluorescent dye (10 mg/ml) for visualization. Cultured media was aspirated from the wells containing devices and cells were washed twice with PBS, then allowed to incubate in the fluorescent dye for ~ 10 minutes prior to the video recording of fluorescent signals along the entire length of the device. At the completion of recording, microchannel devices were peeled from the surfaces of the wells (Fig. 2.2.1) with tweezers, and cells remaining on the peeled devices were recorded and manually counted for yield percentage calculations.

#### **2.2.5 Preparation of whole-cell samples**

Protein samples were prepared by first collecting the cells from culture. Culture media was removed and cells were rinsed twice with PBS. Surfaces of the wells were carefully scraped using a Costar<sup>®</sup> 3010 Cell Scraper (Corning, Inc.) to remove as many 2D cells as possible. Residual cells from the surface were removed by application of 1ml/well of trypsin/EDTA for five minutes at 37<sup>0</sup>C. Cells were retrieved from microchannels by using tweezers to invert the PDMD devices (channel-side-up) to expose the microchannels to trypsinization for 5 minutes at 37<sup>0</sup>C. Residual cells were removed from the microchannels by scraping with an additional scraper. Cells from the two conditions were stored in separate centrifuge tubes and centrifuged at 4000 rpm for 10 minutes, forming a pellet of cells at the bottom of the tube.

#### **2.2.6 Preparation of soluble protein fractions**

To detect specific proteins in the cell extract, total protein extractions were obtained from the cells by incubation with a RIPA lysis buffer (R0728, Sigma-Aldrich) cocktail containing proteinase inhibitors (P2714 Sigma-Aldrich) to prevent proteolytic cleavage. Incubation lasted 30 minutes, followed by centrifugation to remove insoluble cellular debris. Supernatants were collected and quantified using the Pierce<sup>®</sup> BCA Protein Assay kit (Thermo Scientific). The proteins were separated on 10% SDS Page gels, and electrotransferred onto a PVDF transfer membrane (Bio-Rad) with transfer buffer (25 mM Tris, 192



mM glycine, 20% methanol). PVDF membranes were subsequently blocked with a 5% blocking solution of neutral milk proteins, then prepared for probing with target antibodies.

### **2.2.7 Statistical Analysis**

All data represented as average  $\pm$  standard deviation. For each condition, paired t-test was performed by Microsoft Excel to compare the differences in protein concentrations between samples. One-way ANOVAs were performed for comparison of significance differences among the groups. \* = P-Value of 0.05 or less.

## **2.3 Results**

### **2.3.1 Viable migrating cell recovery from PDMS device**

Cells were seeded ( $100 \times 10^3$  cells/device) and allowed to migrate into the microfluidic device for ten days and were periodically monitored, Figure 2.31 A. We found that the amount of cells that could migrate through the microchannels peaked at day 10, before they would begin to die off. The amount of cells that could migrate through the channel was quantified (n=5 devices/6-well plate). Once quantified we peeled the microfluidic device off of the substrate surface (polystyrene) and faced right-side-up to calculate the amount of viable cells remaining in the micro-channels. Our calculations show a 92% recovery of migrating cells after peeling. We successfully demonstrated through our PDMS device the ability to quantify a thousand or more migrating cancer cells both before and after peeling the device.

### **2.3.2 Grouping of migrating from non-migrating cells**

After 10 days of culture, a significant amount of cells was collected and lysed for further analysis. Microfluidic devices were carefully scraped to obtain cells which had migrated through the microchannels. These cells were kept separate from cells which were scraped from the 2D monolayer. A significant amount

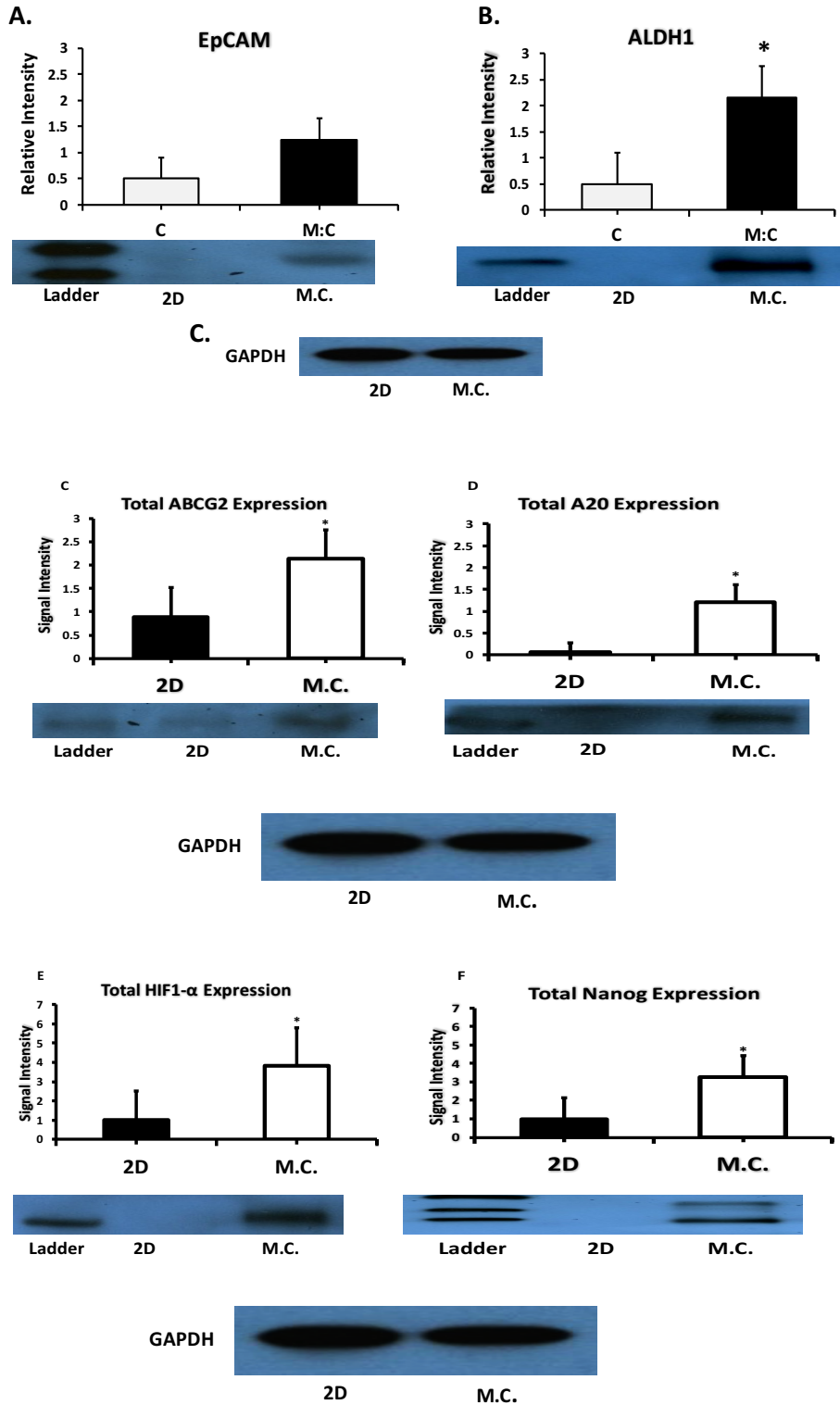
of intercellular protein was obtained for each sample. The efficient recovery of migrating cells from the microchannels during the scraping process made possible this high recovery yield.

### **2.3.3 Western Blot analysis of EMT-related proteins**

While transmembrane glycoprotein, epithelial cell adhesion molecule (EpCAM) expression in migrating breast cancer cells increased only slightly, aldehyde dehydrogenase 1 (ALDH1) expression, an enzyme known to interact with EpCAM in stimulation of EMT, almost doubled in migrating cells.(51) In comparison, expression levels of both proteins were barely detectable in breast cancer cells in the 2D environment, Figure 2.3.A. Membrane transporter glycoprotein, ATP-binding cassette (ABCG2) known for its contribution to drug-resistance and induction of EMT, seemed to increase its expression 2-fold upon migration of breast cancer cells.(41) Zing-finger protein A20 also increased significantly in migrating breast cancer cells, Figure 2.3.D.

Increased expression patterns were also seen in transcription factors, Nanog and hypoxia-inducible factor 1- $\alpha$  (HIF1- $\alpha$ ).(52) Nanog expression increased by nearly 3-fold, while HIF1- $\alpha$  expression increased by nearly 4-fold in migrating breast cancer cells in comparison to non-migrating cells, Figure 2.3.B In contrast to the previously mentioned protein expression changes induced upon migration, fibronectin, a cell adhesion ECM protein displayed decreased expression in migrating cells compared to cells in the 2D environment, Figure 2.3.D.

For MCF7 cells, which represent a hormone positive cancer type, estrogen receptor (ER), and progesterone receptor (PR), increased expression of certain EMT markers was also seen in migrating cells vs. nonmigrating cells. For MCF7 cells, a much less aggressive cancer cell line, ABCG2 increased 2-fold as well, Figure 2.4A. Epidermal growth factor receptor (EGFR), one of the major receptors actively involved in disease progression in hormone receptive cancers, was increased 10-fold in migrating cells in comparison to nonmigrating cells, Figure 2.4B. E-Cadherin, a major tumor suppressor was seen to decrease 30-fold in migrating MCF7 cells in comparison to nonmigrating cells, Figure 2.5.



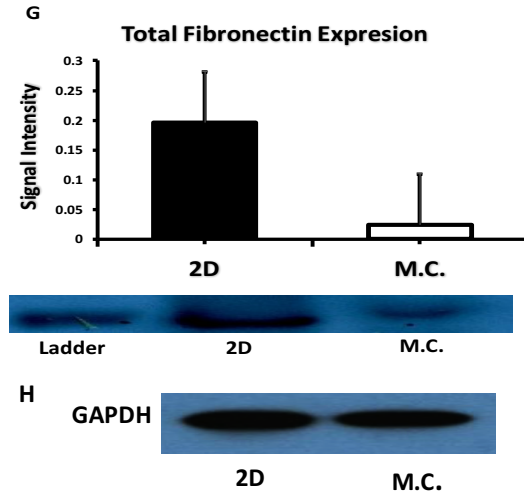


**Figure 2.3** Western Blot analysis of protein expression changes during migration of breast cancer cells. Effect of expression differences in: EpCAM (A), ALDH1 (B), ABCG2 (C), A20 (D), Nanog (E), and Fibronectin upon migration of breast cancer cell migration. GAPDH is the loading control (H). \* $P \leq 0.05$  comparison of microchannel (M.C.) cell expression to 2D (control) cells.

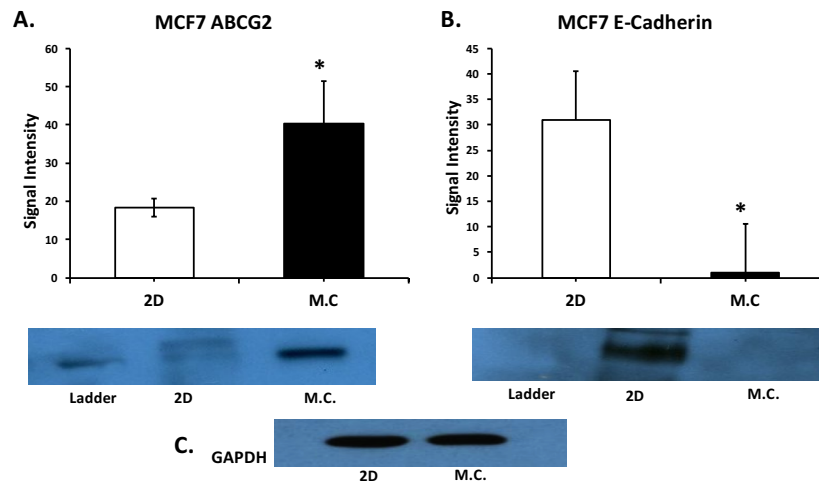


**Figure 2.4.** Western Blot analysis of protein expression changes during migration of a non-invasive breast cancer cell line, MCF7. Effect of expression differences in: ABCG2 (A) and E-cadherin (B) between non-migrating and migrating cells. GAPDH is loading control (C). \* $P \leq 0.05$  comparison of microchannel (M.C.) cell expression to 2D (control) cells.

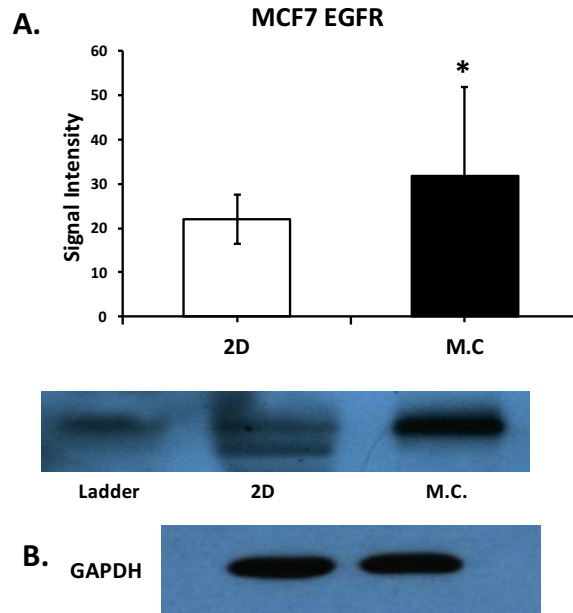


**Figure 2.5. Western Blot analysis of protein expression changes during migration of a non-invasive breast cancer cell line, MCF7.** Effect of expression differences in EGFR (A) between non-migrating and migrating cells. GAPDH is loading control (C). \* $P \leq 0.05$  comparison of microchannel (M.C.) cell

## **2.4 Discussion**

### **2.4.1 Induction of increased EMT stimulating proteins in breast cancer cells**

EMT, a transition cells undergo endowing them with the ability to attach to a substrate, acquire the mobility to migrate to distant sites, and in the case of cancer cells, become invasive by settling at distant sites and begin to differentiate and divide forming new tumors secondary sites. EpCAM is glycoprotein that mediates  $\text{Ca}^{2+}$ -independent, hemophilic adhesions on the basolateral surface of most epithelial cells. It has long been a marker for epithelial and cancer cells.(51) Often implicated in EMT-conversion of breast cancer cells, the increased expression of this protein may likely have played a role in the induction of migration of MDA-MB-231 breast cancer cells. Tumors expressing increased production of EpCAM have been reported to contain subpopulations of highly invasive cancer cells with high expression levels of ALDH1A1. It is believed that these subpopulations are significantly more resistant to platinum treatments, are biologically aggressive, and their expression tends to be associated with a poor patient prognosis.(36) Recent studies

suggest that control of retinoid signaling through ALDH1A1 cancer cell dedifferentiation and chemoresistance are positively correlated with increased expression, making it a biomarker for disease progression.(37)

HIF1- $\alpha$ , a heterodimeric transcription factor is a mediator of the cell's response to hypoxic conditions. Downstream transcription pathways during this time include genes regulating angiogenesis, erythropoiesis, cell cycle, metabolism, and apoptosis. In contrast, this protein is rapidly degraded in normoxic conditions. Additionally, HIF1- $\alpha$  can be induced in an oxygen-independent manner by various cytokines through the PI3K-AKT-mTOR pathway, also a regulator of normal cellular processes, but results in survival and proliferation of tumor cells upon aberrant activation.(38) In addition to inducing increased expression of ALDH1A1, HIF1- $\alpha$  has also been implicated in forming a breast cancer lung metastatic niche by activating the carbonic anhydrase IX-nuclear factor  $\kappa$ B(NF- $\kappa$ B)-granulocyte colony-stimulating factor (G-CSF) axis in breast cancer cells. In this experiment, epigenetic expression of this protein in cells that migrated through the microchannels increased virtually 4-fold in comparison to cells that did not migrate.

Another transcription factor believed to be supremely involved in conversion of breast cancer cells from a stationary epithelial phenotype, to an invasive mesenchymal phenotype is Nanog. While Nanog modulates the stem cell reprogramming of somatic cells, is not expressed in most normal adult tissues. However, it has been found to be overexpressed in many types of human cancers, including breast cancer.(53) Ectopic expression of the protein deregulates the expression of a number of genes associated with tumorigenesis and metastasis. Nanog has been linked to poor prognosis in breast cancer patients.(54) However, it is increasingly being considered as a potential therapeutic target due to the absence of expression in most adult tissues. Expression of this protein was increased nearly 2-fold in migrating breast cancer cells, a strong indication of increased invasiveness activity.(55)

ABCG2 is part of a family of efflux receptors that span the cell membrane six times and can exist as either homo- or heterodimers linked by a short intracellular flexible linker region, which plays an important role in the efflux of a wide range of substrates from the cell.(56) These efflux receptors are believed to be uniquely involved in drug treatment resistance by way of a mechanism it uses to discharge harmful chemicals from the cell, thereby decreasing potency early enough to prevent these chemicals from harming the cell. Expression of this cell surface protein doubled in migrating breast cancer cells. This result may represent the cells' preparation for protection from chemotherapy, or some alternative protective mechanism as relates to anti-apoptosis.

A Cys2/Cys2 zinc finger protein, tumor necrosis factor, alpha-induced protein 3 (TNFAIP3) or A20 is induced by tumor necrosis factor (TNF) and interleukin 1 (IL1) and acts as a negative regulator of NFkB gene expression.(57) By inhibiting expression of this gene, A20 inhibits TNF-induced NFkB activation, and thus inflammatory stimulated cell death. Migrating breast cancer cells increased expression of this protein 8-fold, indicating a possible protective mechanism for cells during disease progression. Fibronectin is a major cell adhesion ECM component which typically plays a role in cell adhesion, migration, differentiation in healthy epithelial cells. Due to its specific functions in the cell, we hypothesized that expression of the protein would increase in migrating breast cancer cells, rendering it more migratory and invasive. The opposite occurred. In a recent study, it was found finding that upregulated expression  $\alpha 5\beta 1$ -integrin and its ligand, fibronectin were positively correlated with malignancy in breast cancer.(58) Cell treatment with a peptide that disrupts the interaction of the two molecules promoted apoptosis in malignant cells, further heightening the apoptotic effects of radiation. Varying expression patterns have also been reported for fibronectin upon induction of EMT.(38) However, our migrating breast cancer cells expressed a statistically significant decrease in the protein, which may be explained by ECM degradation and reorganization which takes place as a result of cells breaking away from the primary tumor site.

It is not surprising to see such aggressive epigenetic changes take place in a TNBC. It is one of the absolute most aggressive forms of cancer. However, TNBC account for ~ 20% of breast cancers.(39) So identifying EMT markers which are pervasive to both aggressive and nonaggressive cancer types opens the door for design of more all-encompassing targeted anticancer therapies. Bearing this in mind, we also migrated MCF7, a hormone receptive and nonaggressive breast cancer cell line for analyses of EMT markers. As with MDA-MB-231 cells, ABCG2 membrane efflux transporter increased by double in expression in migrating cells in comparison to nonmigrating cells, Figure 2.4A. In addition, EGFR expression was increased in migrating cells., Figure 2.4B. Due to the receptor's involvement in disease progression in a broad range of cancer types, this result was not surprising. E-Cadherin expression was decreased to a nearly non-detectable expression level in migrating cells in comparison to nonmigrating cells, Figure 2.5. During EMT, mammary epithelial cells lose these epithelial cell intracellular junctions and cell polarity, while cell mobility increases and leads to disease progression.(40) MCF7 cells grew in culture as epithelial clusters, so a drastic decrease in expression of this protein was to be expected.

## **2.5 Summary and Future studies**

To summarize, we have fabricated a microfluidic device we believe will to help to elucidate major intracellular activities governed by the onset of EMT, including phenotypic modifications breast cancer cells undergo during migration and metastatic invasion of secondary organs. As a response to stress and 3D confinement, we believe the breast cancer cells increased expression of numerous proteins and transcription factors which have previously been linked, to transcriptional reprogramming, motility, and resistance to cell death. Just the same, we suspect that the decreased expression of a major component of the ECM as well as intracellular junctions is indicative of degradation of the basal membrane, and subsequent exposure of these neoplastic cells to the blood and lymph vessels. Future studies should include analysis of the effects these protein expression changes may have on drug resistance. Immunostaining of fixed cell culture samples with the above mentioned proteins may unveil more specific modes of action based on intracellular



compartmentalization of these proteins at different stages of disease progression. Additionally, culture of these cells in a breast tissue biomimetic environment such as a surrounding ECM or underlying basement membrane may unveil additional markers for drug resistance and intravasation that may be lacking in the absence of such tissues.

## **CHAPTER 3: FABRICATION OF AN ENGINEERED BASAL LAMINA EQUIVALENT FOR CANCER CELL RESEARCH**

### **3.1. Introduction**

Breast cancer comprises one of the largest cancer groups in the United States and its metastasis leads to more deaths than most other diseases. Accounting for nearly 1 in 3 cancers diagnosed among women in the U.S., medical expenditures for breast cancer are expected to be \$158 billion, a 27% increase from 2010, according to NIH analysis.(59) Likewise, lung cancer is the leading cause of cancer deaths among men and second leading among women in the U.S. It is also the leading cause of cancer death among men, and second leading cause of cancer death among women worldwide.(59) The development of efficient tools to use for the early diagnosis and effective treatment of cancer is an urgent priority for healthcare.

Studies show that the likelihood of approval from pre-clinical discovery to phase I clinical trial is lowest for oncology drugs (7%) compared to other drugs.(60) One of the reasons for many of these therapeutic failures is the traditional use of conventional 2-Dimensional (2D) petri dish and monolayer cell cultures in the study of non-malignant and malignant cancer cells. With the use of these culture models, cells lose their tissue specific functions and morphological organization. This drastically changes the biology of the cells and makes the researcher unable to recapitulate some crucial inherent characteristics of the tumor, cell migration, and invasion which likely effect responsiveness to therapeutics.(61)

There has been a tremendous increase in the design of biomimetic cell cultures for the study of invasive behaviors of cancer cells. The similarities these cell cultures have with the complex tumor microenvironment as compared with classical monolayer polystyrene cultures, have provided more reliable results when used to screen several forms of anticancer therapy.(62,63) To explore the intrinsic mechanisms cancer cells may utilize to facilitate therapeutic resistance, it is important to use tools that resemble the tumor microenvironment as closely as possible. To provide such tools, it is necessary to understand what constitutes this environment. It is known that epithelial cells are in close contact with the extracellular matrix (ECM), a complex network of non-cellular macromolecules which provide critical biochemical and biomechanical signals to control cell survival, proliferation, and differentiation.(64,65)

The ECM modulates cell morphology acting as a substrate and reservoir for adherence and growth factors respectively. The ECM is connected to the nucleus by a network of protein molecules that include transmembrane adhesion proteins, the cytoskeleton and the nuclear matrix.(65) The matrix networks are different between normal and tumor cells, and modification of the ECM induces alterations in the composition of the nuclear matrix.(66)

Seth *et. al.* demonstrated that ECM proteins protect small cell lung cancer cells from chemotherapy-induced apoptosis, thereby enhancing drug resistance.(67) Loessner *et. al.* demonstrated that ovarian cancer cells displayed unique proliferation characteristics when exposed to ECM as opposed to monolayer plastic culture dish.(62) These ovarian cancer cells also had higher survival rates after exposure to paclitaxel, reflecting similar chemotherapeutic events as seen in patients clinically. Factors required for premalignant progression, growth of primary cancer, invasion and metastasis are all altered by stromal interactions. The basal lamina (BL) is an ultrathin (50-100nm thick) sheet-like structure of extracellular matrix (ECM) which separates cells from connective tissue.(63) The BL is typically found underlying all epithelium and endothelium; some surrounding other cells throughout the body such as muscle, fat, and nerve cells. Within

the BL there are four primary components (collagen type IV, laminin, entactin and perlecan) that uniquely self-assemble and highly crosslink so that the thin BL becomes considerably stable, yet flexible.(68) Those components not only allow the BL to directly contact cells but also provide the BL with the ability to support overlying cells, molecularly filter, and mediate cell to cell communication. BL interruption may occur physiologically during development or immune surveillance. However, in most cases it is from the onset of numerous diseases ranging from fibrosis to malignant cancer.(69)

Herein, a novel material was developed to create uniform, thin membranes (0.5 to 3 $\mu$ m thick) made of collagen type I and ECMgel. Acting as an engineered basal lamina (EBL), this material was utilized to investigate intracellular changes that take place during cancer growth. The material was used in a high throughput screening model to analyze breast and lung cancer cellular responses to anticancer drugs. While ECMgel provided key molecular elements of the EBL (i.e., laminin, collagen type IV, entactin and perlecan), collagen type I incorporation increased its mechanical strength. The fabrication technique was not only simple, Figure 3.1. but also resulted in a unique scaffold to study various cellular behaviors. In fact, given that multiple primary cell types grew well on the EBL, Figure 3.2. we showed its high cell growth supportive properties for *in vitro* applications. Breast cancer cells demonstrated a significant difference in morphology, protein expression, and drug response between EBL coated cultures and classical polystyrene monolayers. Lung cancer cells demonstrated differences in both protein expression and drug response between cell culture types. These results substantiate the need for culture of cancer cells in the context of their natural environment as we strive to uncover valuable molecular, protein, and genetic markers for the effective treatment of cancer.

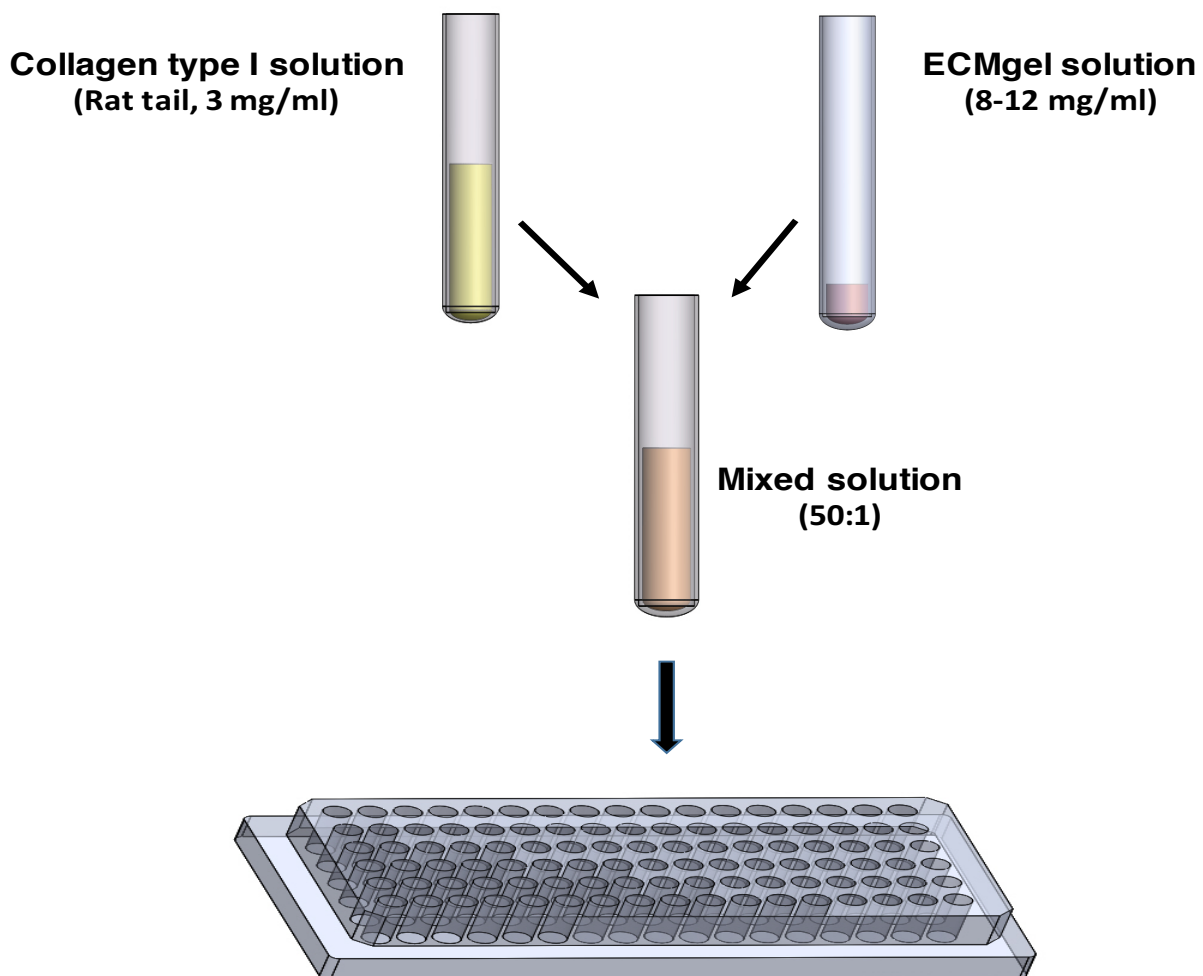


**Figure 3.1. Summarization of fabrication procedure for EBL.** Collagen Type I extracted from rat tail vein was diluted to a 3mg/ml concentration, then mixed with ECMgel at a 1:50 v/v ratio. The mixture was pipetted into appropriate wells of a 96-well plate and allowed to air dry overnight. Subsequently, the samples were crosslinked under UV lamp for 30 minutes and decontaminated by re-exposure to UV light for 20 minutes. Prior to cell culture, the samples were rinsed three times with phosphate buffer saline (PBS) to neutralize the acidity of the collagen.

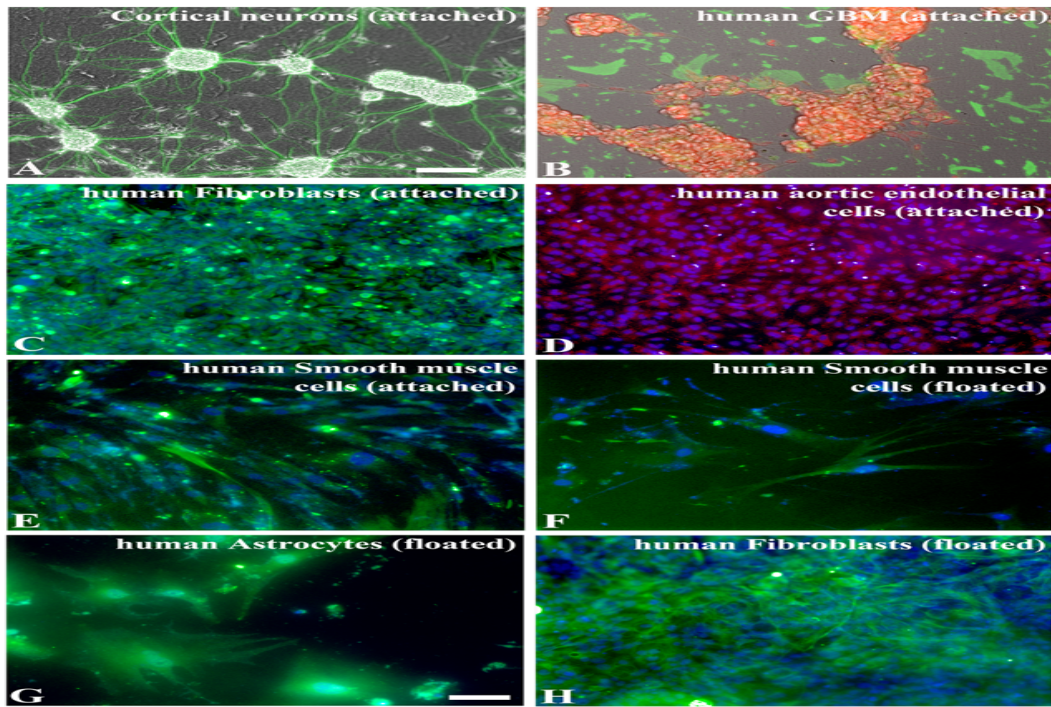


**Figure 3.2. Applications of the EBL for cell culture.** (A) E-18 derived rat cortical neurons cultured on EBL (Phase and beta III tubulin, green). (B) Primary human Glioblastoma multiforme (GBM) cells cultured on the EBL and stained for EGFR (red) and laminin (green). (C) Human glioblastoma cells on the basal lamina membrane were fixed and stained for laminin (green) and EGFR (red). (D) Human aortic endothelial cells cultured on the EBL and stained for VWF (red) and nucleus (DAPI, blue). (E) Human smooth muscle cells were cultured on the membrane attached on glass. The cells were fixed and stained for smooth muscle actin (green) and nucleus (DAPI-blue). (F) Human smooth muscle cells, human astrocytes and human fibroblasts were also cultured on the floating basal lamina membrane and were stained for smooth muscle actin and nucleus (DAPI – blue). (G) Human astrocytes were stained for glial fibrillary acidic protein (GFAP) (green). (H) Human fibroblasts were stained for Vimentin (green) and nucleus (DAPI – blue).

## **3.2 Methods**

### **3.2.1 Fabrication of the Engineered Basal Lamina Equivalent (EBL)**

Fabrication procedure for EBL was summarized in Figure 3.1. Collagen type I (3mg/ml), pre-collected from rat tail vein as described previously,(70) and ECMgel (8-12mg/ml, Sigma) were mixed at a 1:50 v/v ratio. In the original design, the mixture of Collagen Type I and ECMgel was then spread on the PDMS mold followed by approximately eight hours of air flow through a customized tunnel. Once air dried, the EBL was placed under a UV lamp (UVP Blak-Ray® B-100AP; 100W, 365nm) for 25 minutes to crosslink the proteins, and then allowed an additional 60 minutes to sit before peeling off from the PDMS mold. The EBL maintained its mechanical properties after peeling off. In a subsequent and more efficient design, a liquid mixture of the collagen and ECMgel was pipetted directly into the wells of a 96-well plate then crosslinked under the UV lamp for 30 minutes, Figure 3.1. Prior to cell culture, the membrane was decontaminated by re-exposing to UV light in the bio-safety cabinet for 20 minutes, then rinsed three times with PBS.

### **3.2.2 Material Characterization of EBL**

By adjusting the mixture volume (50, 100, 150, and 200 $\mu$ l) ( $n \geq 3$  per each mixture volume), we evaluated the range of the EBL thickness by using profilometer (Alpha Step IQ profilometer). Their mechanical properties were examined ( $n=5$  per each mixture volume) using MTS Insight machine. One-way ANOVA was performed to compare among the groups. We then chose the membrane fabricated from 100 $\mu$ l mixture as a representative for further experiment. For analysis, the EBL was fixed with 4% paraformaldehyde and double immunostained for laminin (RbIgG, 1:500, Sigma) and collagen type I (mIgG1, 1:200, Sigma). Surface topography of the EBL was examined by using a Dimension 5000 atomic force microscope (AFM) ( $n=6$ ) and a Zeiss Supra 55VP scanning electron microscope (SEM, Carl Zeiss).

### **3.2.3 Cell Cultures**

Eight different cell types used in our study included human aortic endothelial cells (HAEC), human aortic smooth muscle cells (HASMC), human fibroblasts, glioblastoma multiforme (hGBM), E-18 derived rat cortical neurons, human astrocytes, A549 human small cell lung cancer cells, and MDA-MB-231 breast cancer cells. All human cells were provided by The University of Texas at the Southwestern Medical Center in Dallas. HAEC, HASMC, human fibroblast, and astrocytes were cultured in DMEM/F-12 medium containing 10% fetal bovine serum. hGBM cells were cultured in serum-free tumor medium DMEM/F-12 supplemented with B-27 (Invitrogen), Insulin Transferrin Selenium-X (Invitrogen), gentamycin (50 $\mu$ g/ml; Invitrogen), 20ng/ml mouse epidermal growth factor and 20ng/ml basic fibroblast growth factor. E-18 derived rat cortical neurons were cultured in Neurobasal medium supplemented with B-27, gentamycin, and L-glutamine. A549 lung cancer cells were cultured in Roswell Park Memorial Institute (RPMI) 1640 medium (Corning/Cellgro) supplemented with 5% fetal bovine serum. MDA-MB-231 breast cancer cells were cultured in DMEM/F-12 medium (Corning/Cellgro) supplemented with 10% fetal bovine serum.

### **3.2.4 Breast cancer Cell Culture on EBL**

EBL films were fabricated by 40 $\mu$ l of the liquid film being pipetted directly into the wells of a 96-well plate, allowed to dry overnight, crosslinked in a laminar-flow hood under UV lamp (long-wave/350 nm) for 30 minutes, and decontaminated by re-exposure to UV (200 nm) in Biosafety cabinet for 20 minutes. Prior to cell seeding, films were rinsed three times with PBS and last rinse remained for 10 minutes to neutralize acidity from the collagen. 3 $\mu$ l of A549 lung cancer cells, and 3 $\mu$ l of MDA-MB-231 breast cancer cells were pipetted into the wells of their respective plates, followed by 200 $\mu$ l of their respective culture media (see Cell Culture). Cells were cultured on the films for roughly 4 days.

### **3.2.5 Quantification of Cancer Cell Protein Expression by Western Blot**

Briefly, whole cell lysates were prepared using RIPA buffer (R0728, Sigma-Aldrich) and proteinase inhibitors (P2714 Sigma-Aldrich). Supernatants containing concentrated whole cell protein were isolated and quantified to determine sample concentrations using the Pierce® BCA Protein Assay kit (Thermo Scientific). The proteins were separated on 10% SDS Page gels, and electrotransferred onto a PVDF transfer membrane (Bio-Rad) with transfer buffer (25 mM Tris, 192 mM glycine, 20% methanol).

PVDF membranes were blocked with 5% powdered non-fat milk. Monoclonal antibodies used were Integrin- $\beta$ 1 (4706S, Cell Signaling), E-Cadherin (24E10 Cell Signaling), Focal adhesion protein (FAK) (Cell Signaling), Epidermal growth factor receptor (EGFR) (D38B1 Cell Signaling), Vimentin (MA5-11883, ThermoFisher), b-tubulin (TU-20, Cell Signaling), c-MET (25H2, Cell Signaling), and GAPDH (HRP-60004, Proteintech

### **3.2.6 Viability Analysis**

MTS cell viability assay (Promega CellTiter 96® AQueous) was performed. Briefly, cell samples were incubated with varying chemotherapeutic drugs of increasing concentrations, for 24 hours. Table 3.1. Subsequently, the samples were introduced to an MTS reagent, then incubated at 37<sup>0</sup> C for 2 hours. Absorbance was measured by spectrophotometry at 490 nm.

### **3.2.7 Immunostaining**

72 hours after cell seeding, the cell containing EBLs were fixed with 4% paraformaldehyde in 1xPBS and immunostained for the following markers: Von Willebrand factor (VWF, RbIgG, 1:200; Santa cruz biotech) for HAEC; Smooth muscle actin (mIgG2a, 1:200; AbDSerotec) for HASMC; Vimentin (mIgG1, 1:500; Sigma) for human fibroblasts; GFAP (RbIgG, 1:1000; Dako) for human astrocytes; EGFR (mIgG2b, 1:500; Sigma) for hGBM; and class III  $\beta$ -tubulin (mIgG2b, 1:500; Sigma) for cortical neurons.



## **3.3 Results**

### **3.3.1 Characterization of EBL**

Using the fabrication technique in Figure 3.1., we successfully assembled an EBL with a thickness ranging from approximately 0.5 – 3  $\mu\text{m}$ . Evaluation of the mechanical properties of the film resulted in no significant difference in strain at break or peak stress among multiple films, Figure 3.3(A, B). As the mixture volume increased, the young modulus decreased, indicating that the membrane became more elastic. This was quite consistent with the breaking strain results: 100ul mixture resulted in higher breaking strain compared to 50ul.

Immunostaining resulted in visualization of the presence of both laminin and collagen type I uniformly distributed over the film, Figure 3.3C. AFM measurement based on readings between two random points of the EBL demonstrated a submicron texture of  $156.88 \pm 42.59\text{nm}$ , Figure 3.3D. Moreover, results from SEM showed a uniformity of EBL surface topography, Figure 3.3E.

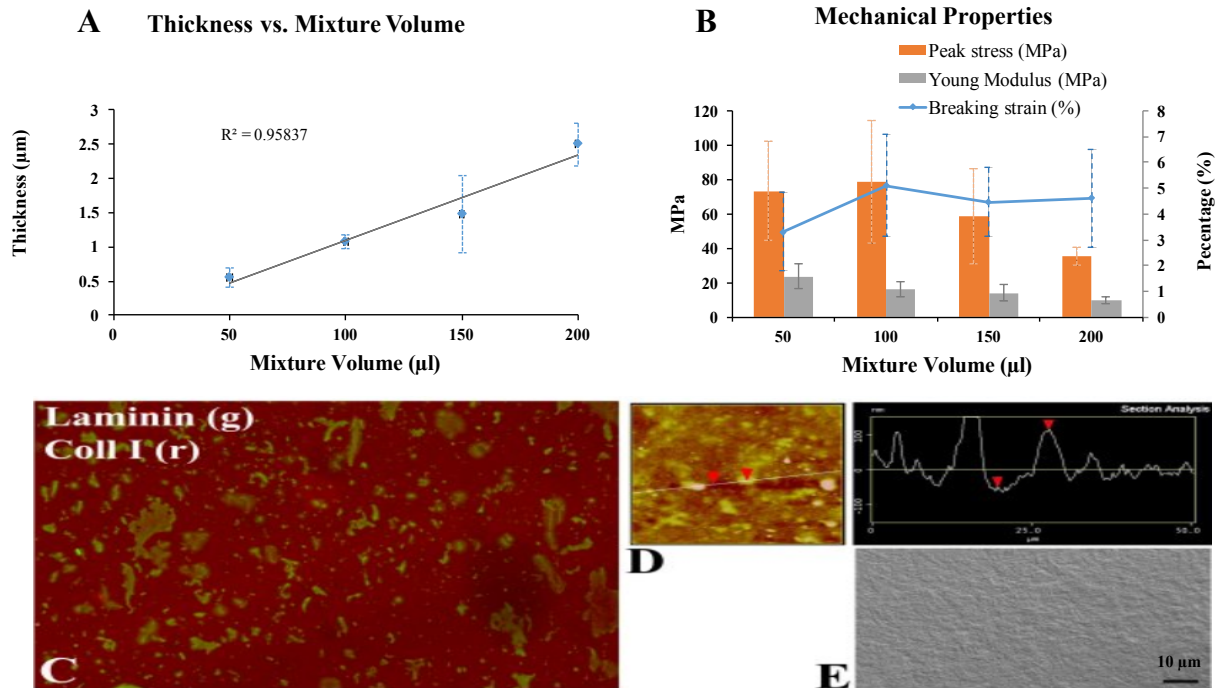


**Figure 3.3. Characterization of the Engineered Basal Lamina.** (A) EBL thickness for 4 different volumes of substrate mixture. (B) Mechanical properties of EBLs with 4 different mixture volumes. (C) Fluorescence image of lamina (green) and collagen type I (red) expression on EBL surface. (D) AFM results of surface nanostructure. (E) SEM image of surface topography. Scale bare = 10 μm.

### 3.3.2 Robust growth of different cell types on EBL

We demonstrated that EBLs were highly cell growth supportive for six different cell types, Figure 3.2. Immunostaining yielded positive staining for selected markers, revealing a high density (more than 50% confluence) of viable cells cultured on the film. All cell types remained in their well-adhered morphologies with multiple elongated process and presented abundant connections to each other. For example, E-18 rat derived cortical neurons showed numerous neurite extensions via class III β-tubulin; HASMCs were in their bipolar shapes and well aligned to one another; HAECs and human fibroblasts had a high proliferation capacity on the film and formed sheet-like structures.

### **3.3.3 Western blot analysis of protein expression in breast cancer cells culture on EBL**

E-cadherin, a transmembrane glycoprotein involved in calcium-dependent cell to cell adhesion and normal tissue development was expressed slightly less in MDA-MB-231 cells grown on the EBL than those grown on the polystyrene plate, Figure 3.4A. Vimentin expression was expected to be disparate between breast cancer cells grown on the EBL and those grown on the polystyrene, Figure 3.4B. This is due to the protein's significant role in onset of EMT and disease progression in breast cancer.(71) In our study however, expression of Vimentin remained relatively stable between the two surfaces.  $\beta$ -tubulin, on the other hand increased almost 2-fold in expression from the ELB to the polystyrene, Figure 3.4C. As a major protein involved in cellular mitosis and microtubule assembly in the nucleus during cell division, we didn't expect to see a significant difference in expression patterns among highly invasive breast cancer cells grown between the two surfaces. Focal adhesion kinase (FAK) is a widely expressed cytoplasmic protein tyrosine kinase involved in integrin-mediated signal transduction.(72) It plays an important role in the control of several biological processes, including cell spreading, migration, and survival. FAK protein expression was increased slightly, but overall remained stable in expression patterns of cells grown between the EBL and polystyrene surfaces, Figure 3.4D. The same expression pattern was seen with Met, a transmembrane receptor-like protein associated with hepatocyte growth factor ligand, Figure 3.4E. The truncated cytoplasmic region of the protein has constitutive kinase activity and is oncogenic.(73,74)

## Protein Expression In Breast Cancer Cells

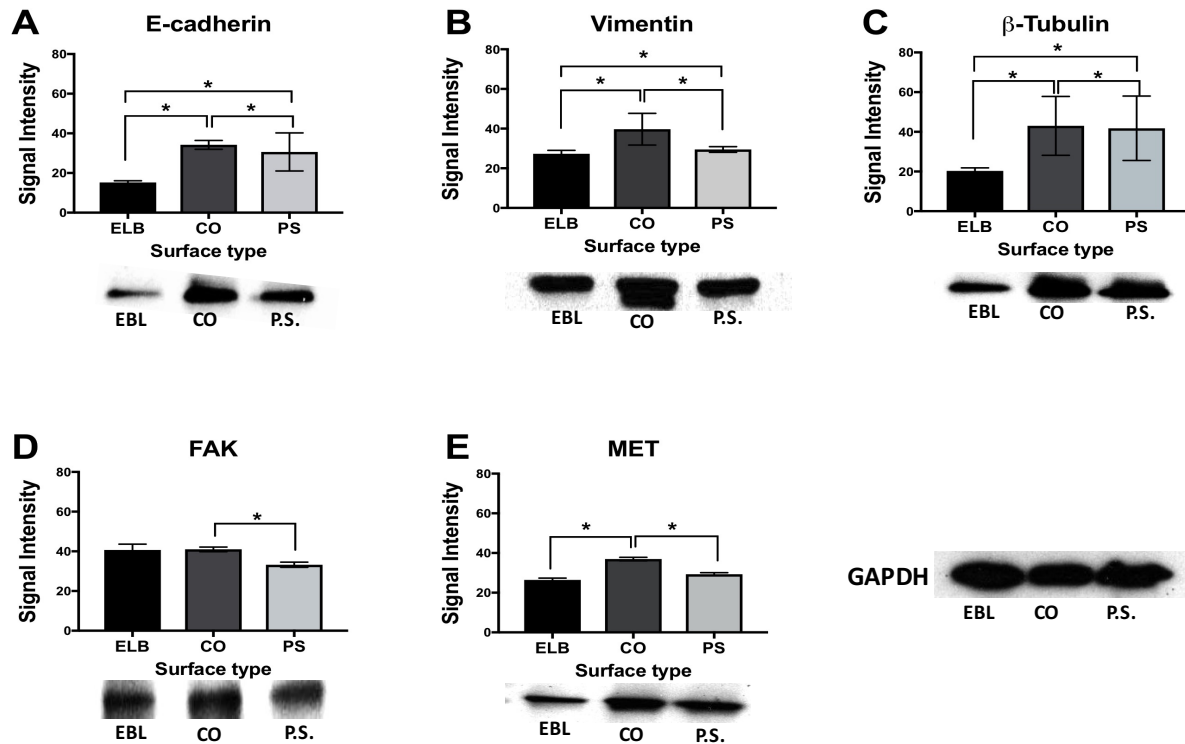


**Figure 3.4. Western Blot analysis of protein expression changes in breast cancer cells among the three cell culture conditions.** Effect of expression changes in: E-cadherin (A), Vimentin (B),  $\beta$ -Tubulin (C), FAK (D), MET (E). \* $P < 0.05$  comparison of M.C. protein expression and P.S (polystyrene) protein expression, to 2D (control) cells. GAPDH: housekeeping protein.

### 3.3.4 Western blot analysis of protein expression in non-small cell lung cancer (NSCLC) cells culture on EBL

Expression patterns for Vimentin, E-cadherin, and Met were distinctly different in lung cancer cell line, A549. Vimentin expression was slightly higher in cells grown on the polystyrene than those grown on the EBL, Figure 3.5A. E-cadherin expression was significantly higher in cells grown on the EBL as compared to cells grown on polystyrene surface, Figure 3.5B. And, MET expression was significantly higher in cells

on the polystyrene than cells grown on the other two surfaces, Figure 3.5C. Epidermal growth factor receptor (EGFR) amplification has been implicated many times in breast and lung cancer progression with a positive correlation to metastasis and poor prognosis.(75–78) In our study, though Met expression was lowest in cells grown on the EBL and highest on the polystyrene plate, the exact opposite of patterns was seen with EGFR expression, Figure 3.5D. This could possibly represent communication between the two receptors in A549 cells and lung cancer. Integrin beta-1, an adhesion molecule regulates a diverse array of cellular functions crucial to the initiation, progression, and metastasis of solid tumors. Han *et al.* demonstrated that increase expression of certain integrins, including Integrin beta-1 and lost expression of collagen matrices significantly correlated with lymph node metastasis of NSCLC.(79) Integrin beta-1, while barely detectable in cells grown on the EBL, was significantly more prominent in expression levels for the polystyrene coating and collagen only film as well, Figure 3.5.E.

Interesting to note is the absence of striking differences in expression patterns of the proteins we specifically targeted on the Western Blot membrane for breast cancer cells. Though there were differences in expression, we certainly expected to see more pronounced differences such as those we saw with lung cancer cells. This is due to the striking difference in total protein expression between the EBL and other two conditions that was seen in over-exposed x-ray film used to visualize protein transfer to the polyvinylidene difluoride (PVDF) membrane, Figure 3.6. Based on the molecular weights, we suspect that specific protein bands that are present in the EBL sample may be related to the inhibition of anoikis: Ki67 (358 kDs); Fox03 (80 kDs); and CD44(70-140 kDs); to name a few. It has been shown that metastatic tumor cells are often able to avoid this anchorage-dependent cell death in order to invade other organs.(79–81) A possible future study to explore targeting of these and other specific proteins involved in this process may yield interesting and pivotal results.

### Protein Expression In Lung Cancer Cells

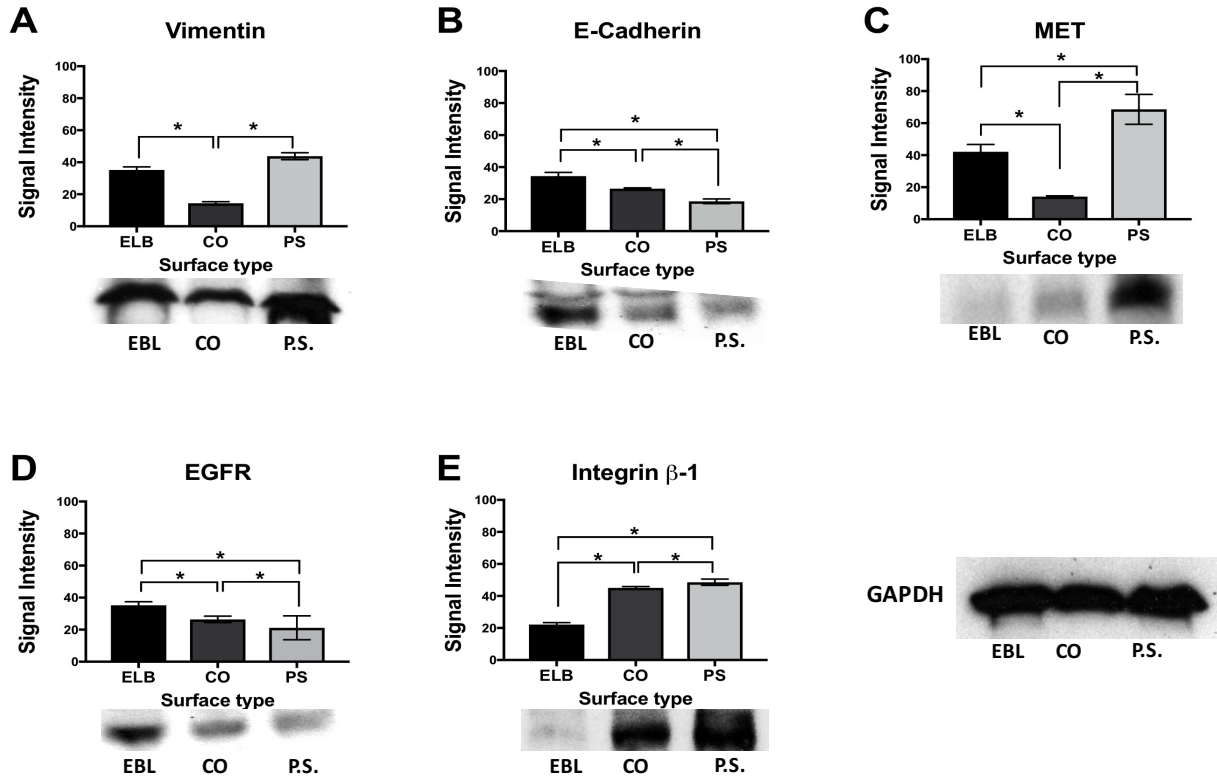


**Figure. 3.5. Western Blot analysis of protein expression changes in Lung cancer cells among the three cell culture conditions.** Effect of expression changes in: Vimentin (A), E-cadherin (B), MET (C), EGFR (D), Integrin  $\beta$ -1 (E). \* $P < 0.05$  comparison of M.C. protein expression and P.S. (polystyrene) protein expression, to 2D (control) cells. GAPDH: housekeeping protein.

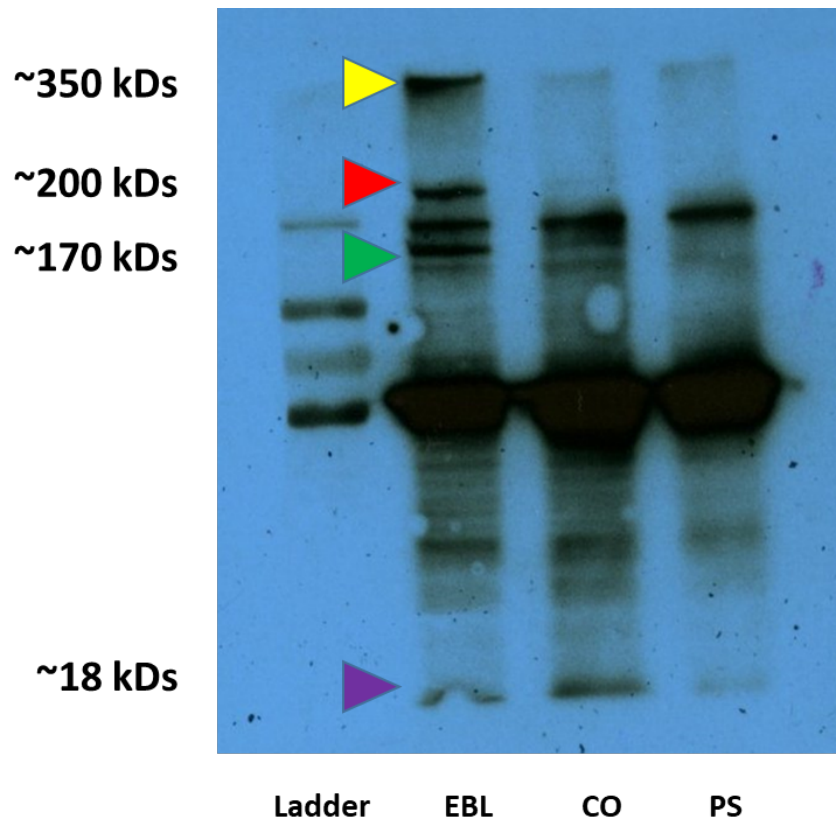


**Figure. 3.6 Over-exposed x-ray film used to visualize Western Blot cell protein transfer in breast cancer cells.** X-ray film shows total cell protein due to over-exposure. Arrow-heads demonstrate striking differences in expression patterns between the EBL and other two surfaces.

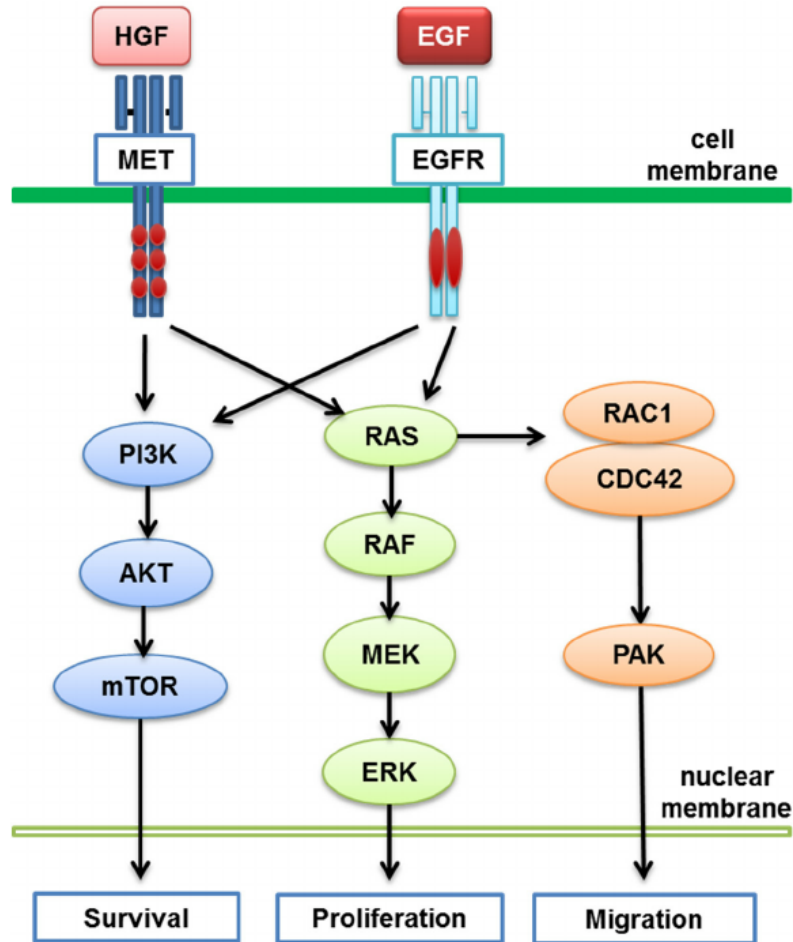


**Figure. 3.7 Metastatic transcriptional crosstalk between MET and EGFR receptors in breast and lung cancer.** MET and EGFR receptors become both upregulated and constitutively activated during cancer migration. Each receptor activates its own downstream cascades, while also stimulating activation of signaling pathways of the other (cross-talk) for enhanced transcription of invasive properties. (82)

### 3.3.5 Drug response of breast and lung cancer cells after chemotherapy

Drug responses for both types on the 3 different surfaces is summarized in Table 3.1. For breast cancer cells, both Dox and TMZ drugs were tested. For lung cancer cells, TMZ was tested. Breast cancer cells displayed a significant difference in cell viability between all three surfaces (trend: **highest on EBL surface**, lowest on polystyrene) for DOX at the 1 micromolar concentration and a significant difference



between all three surfaces for TMZ at the 1000 micromolar, the highest concentration for each respective drug, Figure 3.8. Lung cancer cell viability was significantly different for TMZ (trend: **higher on PS surface**, lower on the EBL) at the 250 micromolar and 500 micromolar concentrations. For the 250 micromolar concentration, the significant differences were found between the PS and EBL surfaces, as well as between collagen only and EBL. At 500 micromolar concentration, the significant difference was found between collagen only and polystyrene, as well as polystyrene and EBL.

<b>Cancer type</b>	<b>Drug</b>	<b>Concentration 1</b>	<b>Concentration 2</b>	<b>Concentration 3</b>
<b>Breast (MDA-MB-231)</b>	Dox	0.25 $\mu$ M	0.50 $\mu$ M	1 $\mu$ M
	TMZ	250 $\mu$ M	500 $\mu$ M	1000 $\mu$ M
<b>Lung (A549)</b>	TMZ	250 $\mu$ M	500 $\mu$ M	750 $\mu$ M

**Table 3.1 Clinically relevant drug treatments for breast and lung cancers.** Breast cancer cells were treated with both Dox and TMZ, each at three increasing concentrations. Lung cancer cells were treated with TMZ at three increasing concentrations.

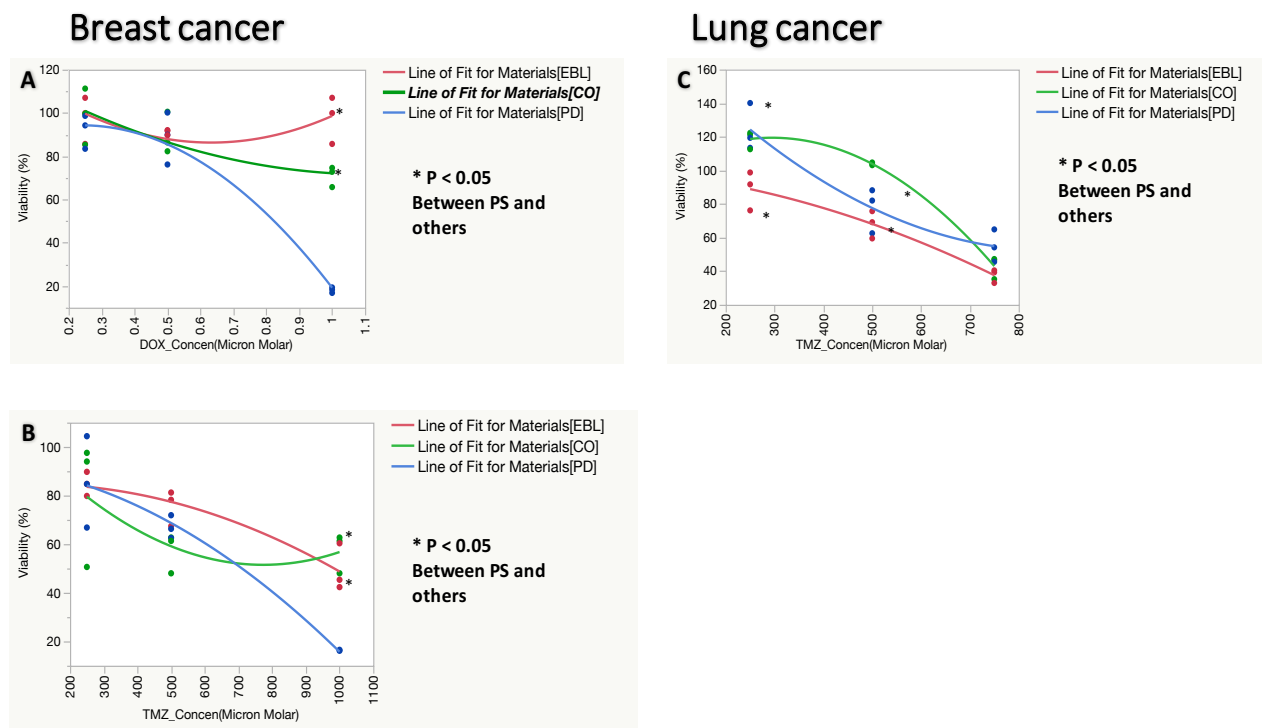


**Figure 3.8 Increased drug resistance for invasive breast and lung cancer cell lines on EBL vs. collagen only film, and polystyrene.** Effect of cell viability after Dox treatment of breast cancer cells (A) and TMZ (B). Effect of cell viability after TMZ on lung cancer cells (C). \*P<0.05 comparison of viability between polystyrene and other conditions.

### 3.4 Discussion

Regardless of their ability to allow cell growth, the conventional plastic and glass substrates might not be compatible to some experimental modalities.(83–85) Importantly, they fail to provide a semblance of the ECM microenvironment, which likely results in loss of innate cellular behaviors. Monolayers of cell growth lack the physical and chemical cues that underlie their function and identity *in vivo*.(86,87) EBLs, on the other hand, might provide the cells with a more compatible environment that more closely mimics that of *in vivo* conditions, thereby reducing the risk of fallible consequences. Furthermore, a scaffold that is able

to support tissue like structures is very important in the field of tissue engineering.(87,88) Some studies have shown the potential of using a substitute of basement membrane in skin tissue engineering. Given such mechanical and biocompatible properties, the EBLs might be involved in further *in vitro* research.(89,90) For example, the membranes may be utilized to mimic the basement membranes of blood vessels for the study of angiogenesis and cancer metastasis. They may also serve as a model for the human blood brain barrier (BBB) in drug delivery studies. The unique nature of the basal lamina (BL) has been reported in many studies.(91,92)

Here, we have developed and engineered basal lamina (EBL) equivalent, which consisted of BL like composition and possessed uniform topography, micron/submicron scale thickness, high mechanical strength, as well as cell growth supportive properties. Immunostaining for collagen type I and laminin was used to show that the proteins did not denature during the engineering process, Figure 3.3C. These membranes, after being air-dried and UV cross-linked, were mechanically strong enough for further configuration and handling. The transparency and thinness of the membranes allowed them to be easily sterilized using UV light. This sterilization limited the use of ethanol and was confirmed to be effective as no contamination was found. By culturing eight different cell types on the EBLs, we also confirmed its cell supportive properties to various cells, Figure 3.2(A-H). EBLs could provide a novel platform for many *in vitro* assays. In a subsequent culture design, the material was allowed to air dry directly in the wells of a 96-well plate, instead of being peeled, for more efficient cellular attachment.

In this study, we utilized the EBL to assay protein expression disparities that may occur between cells grown on the EBL vs. cells grown on the classical polystyrene culture dish. In conjunction with this assay, we also used the EBL to assay chemotherapeutic drug responses of both breast cancer cells and lung cancer cells, and correlate the cellular responses between the two assays. In breast cancer cells, the most significant difference in protein expression between the EBL cell culture and classical polystyrene cell culture was demonstrated by  $\beta$ -tubulin, Figure 3.4C with higher expression seen in cells grown on the classical PS

surface. Due to the protein's involvement in formation of microtubules, it is not wholly unexpected that this would be the case, considering the number of studies which have confirmed that cancer cell proliferation tends to be more aggressive on PS monolayer cultures in comparison to cells grown on ECM films or in 3D cultures.(93,94)

E-cadherin expression between cells grown on the EBL and those grown on polystyrene failed to be significantly different. E-cadherins are found in adherens junctions, a cellular structure in polarized epithelial cells. They are considered an acting suppressor of invasion and growth of many epithelial cancers.(95) Therefore, it is not entirely surprising to see even an inconspicuous decrease in EBL expression in comparison to that of PS. Vimentin is an intermediate filament aggressively involved in dynamic structural changes and spatial organization in response to extracellular stimuli, by coordinating various signaling pathways.(64) *Vuoriluoto et al.* showed that Vimentin expression is necessary for EMT-associated migration, and its knockdown causes a decrease in genes linked to breast cancer cell migration and invasiveness.(64) Based on these findings, it was expected that there would be a significant increase in expression for cells grown on a more aberrant substrate such as the PS. What's interesting to note is that significant changes in expression of Vimentin as well as the other proteins mentioned seem to take place on the collagen only surface, Figure 3.4B. This could be a mild representation of cell response to the breakdown of the basement membrane by degradation of proteins.

Many studies have demonstrated that ECM proteins protect cancer cells from chemotherapy-induced apoptosis, thereby increasing drug resistance.(96) Typical monolayer polystyrene cultures show drastically higher sensitivities to chemo- and radio-therapies than do tumor cells clinically.(97) Due to the overall elevated levels of resistance to chemotherapy detected in tumors clinically and *in vivo* in comparison to 2D monolayers, we initially presumed that we would see a similar trend in our experiment resulting in increased resistance with cells grown on the EBL vs. those grown on the PS. This appeared to be the case for breast cancer cells, likely owing the increase in resistance to the presence of BL proteins and their regulatory

interactions with the overlying cell membranes. Interestingly, breast cancer cells have been known to express a mutation of the  $\beta$ -tubulin gene as an evolved mechanism underlying paclitaxel resistance. Studies have identified this  $\beta$ -tubulin gene mutation as being present both before and after Paclitaxel treatment.(65) Because Paclitaxel is an antineoplastic drug which binds to the  $\beta$ -tubulin subunits on the microtubule, it works to block cells from entering the G2/M phase of mitosis, leading to cell death. However, structural alterations of the protein could modify Paclitaxel sensitivity.(98) Increased expression of the protein in cells on the polystyrene surface could represent one of two possibilities: a) either cellular division was more prolific on the polystyrene surface, or b) cells on the polystyrene surface have augmented their mode of  $\beta$ -tubulin synthesis as a mechanism for protection from apoptotic cell death. If such a correlation exists, it is not yet clear.

The opposite trend of decreased cell viability was seen on the EBL surface in comparison to PS with lung cancer cells, Figure 3.8. The most significant protein expression differences in lung cancer cells grown on the three surfaces were in Met, EGFR, and Integrin  $\beta$ -1, Figure 3.5. Because both Met and EGFR amplification has been shown to contribute to disease progression in lung and breast cancer by cross-talk communication(75) it is interesting to see completely opposing expression patterns for each among the three conditions. It has been shown that each receptor increases inhibition of apoptosis, drug resistance, and invasion of cancer cells by supplemental amplification of the other receptor to compensate for inhibition of its own. It is possible that lung cancer cells grown on the EBL amplified expression of EGFR in an attempt to increase resistance to the drug, Figure 3.5D. In contrast, it may be Met amplification that was more actively involved in the increased cell survival for cells grown on the PS, Figure 3.5C.

In terms of Integrin  $\beta$ -1, the significant increase in expression of the protein in cells grown on PS in comparison to the EBL film was expected considering the protein's role in inhibition of apoptosis.(99) Because drug resistance was higher in cells on the polystyrene than on the EBL, it makes sense that Integrin  $\beta$ -1 expression was also higher in cells on the PS. A look deeper into the specific downstream transcription

cascades that are activated and responsible for expression levels of this protein in correlation to the underlying substrate may uncover an interesting role for the protein in drug resistance. Future studies may include immunostaining of cancer cells to expose subcellular compartmental changes these proteins undergo at distinct stages of disease progression. This may elucidate correlations that exist between cell protein expression and cellular response.

In conclusion, we have designed an EBL that stimulated cell-microenvironment interactions which resulted in specific EMT – related protein expression changes in both breast and lung cancer cells. These interactions also influenced a difference in drug sensitivities to clinically relevant drugs, for both cancer cell types. Based on the resulting trends of drug resistance seen in cells grown on the EBL in comparison to those grown on classic PS surfaces, it is plausible to correlated the divergent EMT protein expression in cells grown on the EBL with this drug response. Due to the overall trend of increased drug resistance documented for tumors clinically and cells grown in 3D vs 2D monolayer cultures, it has become progressively critical that the scientific community develop and utilize tools more efficient in studying the innate phenotypic changes cancer cells undergo in resisting anticancer therapies. This knowledge may aid in a transition to the development of more targeted and effective anticancer therapies.

## **CHAPTER 4: IDENTIFICATION OF CANCER STEM CELL MARKERS IN CELL POPULATIONS AFTER MIGRATION**

### **4.1 Introduction**

Though it has been shown that cancer cells display EMT activities during the process of reprogramming to endow invasive cells with the capacity to invade the circulation and other tissues, we believe that these activities are inducible. Through mechanical stresses imposed upon the cells by confinement, we have demonstrated the ability to stimulate neoplasticity in cancer

cells which transcribes a systematic silencing and activation of gene expression changes that reprogram the cells and protect them from cancer treatment completely during their journey to distant sites. Based on increased expression of stem cell markers, demonstrated with both western blot and immunostaining, we believe mechanical stress and 3D confinement has transformed these cells into cancer stem cells (CSCs). Breakthroughs in research have allowed the characterization of malignancies according to their unique gene expression, which has allowed the pragmatic targeting of many cancer types based on their specific gene expression patterns. For example, trastuzumab improves the overall and progression-free survival in human epidermal receptor 2- (Her2-) positive breast cancer.(100) The receptor-specific monoclonal antibodies bevacizumab and cetuximab have shown remarkable outcome in vascular growth factor receptor- (VEGF-) positive and EGFR-positive cancer, respectively.(101) Overall, these individualized profiling and targeted systems have provided novel tools to improve both prognostic accuracy and individualized treatment for patients. However, our continued inability to target and treat the spread of cancer is a direct result of our failure to consider the plasticity of these migrating cells when designing targeted treatments. A better understanding of the mechanisms that underlie CSC resistance to therapy is necessary. Through acquired capabilities such as resistance to anoikis, oncogene-induced senescence, exposure to chemotherapy, alterations in DNA repair, and cell dedifferentiation, we believe that cells physically safeguard themselves from therapies as well as the harsh environment of the circulation, while possibly reprogramming once again, and undergoing mesenchymal-to-epithelial transition (MET) upon reaching a destination and resettling.(102) Importantly, these nuclear drivers of EMT seem to be involved in both differentiation and dedifferentiation, and this implies that their function is compatible with both growth suppression and stimulation, depending on the context.(103) There is good evidence to

support the idea that dedifferentiation is triggered if the balance between different regulatory networks is fundamentally disturbed. Herein, we report significant upregulation of CSC markers and their correlation with complete chemotherapy resistance in cancer cells. We succeeded in defining protein expression pattern changes these migrating cells undergo even after resettlement into a 2D environment. We believe that the chemoresistance that has been demonstrated in cancer cells upon migration has a distinct correlation with the specific protein patterns that distinguish them from non-migrating cells. We believe these findings may establish our system as an appropriate high throughput screening method for metastatic therapeutic efficacy.

## **4.2 Materials and methods**

### **4.2.1 Fabrication of device**

The microfluidic devices were assembled by utilizing soft and standard photolithography. In order to construct microchannels with 5 $\mu$ m by 5 $\mu$ m height and 15 $\mu$ m by 15 $\mu$ m width, an SU-8 photoresist was utilized to photopattern a silicon wafer. Polydimethylsiloxane (PDMS) was cured at a ratio of 10 (PDMS) :1 (curing agent) in order to activate solidification of the polymer. This mixture was heated at an initial 750C to dissolve bubbles. Subsequently, it was baked at 150<sup>0</sup>C to obtain a solid PDMS mold to peel and expose open microchannels. The microchannels were opened by hole-punching the center cell seeding reservoir and 6 satellite chambers. Devices were subsequently blotted to remove debris from the microchannels. Devices were then sterilized with 70% ethanol, then assembled microchannel-side-down onto glass microscope slides and plasma treated for permanent adherence.

### **4.2.2 Cell culture**

Breast cancer cells were donated by University of Texas Southwestern, and prostate cancer cells were kindly donated from Dr. Kytai Nguyen's lab, University of Texas at Arlington. Human breast cancer cell lines, MDA-MB-231 and MCF7 were maintained in DMEM/F-12 medium supplemented with 10% fetal



bovine serum. Prostate cancer cell line, PC3 was maintained in Roswell Park Memorial Institute (RPMI) 1640 medium (Corning/Cellgro) supplemented with 5% fetal bovine serum. Prior to cell seeding, microchannel devices were coated overnight with collagen overnight, and subsequently rinsed 3 times with PBS. Cells cultured at  $20 \times 10^3$  cells at each of 6 sets of microchannel entrances in the seeding reservoir of the flower device and maintained for  $\sim 7$  days to obtain the highest number of migrating cells.

#### **4.2.3 Cell harvesting for western blot**

Cells from the 2D well surfaces were collected by thoroughly scraping with a Costar® 3008 Cell Lifter (Corning, Inc), and isolated for centrifugation at 4000 rpm for 10 mins. Migrating cells were collected from the microchannels of the devices by trypsinization for 5 mins, then scraping, followed by centrifugation at 4000 rpm for 10 mins. Subsequently, cells from each condition were lysed for protein collection and quantification.

#### **4.2.4 Western blot**

Total cell lysates were obtained by adding RIPA buffer (R0728, Sigma-Aldrich) and protease inhibitor cocktail (P2714, Sigma-Aldrich). Equilibrated protein samples were loaded into and 10% SDS-Page gel and electrophoresed and electrotransferred to a PVDF membrane (Bio-Rad) thereafter. Transfer membranes were blocked with 5% powdered non-fat milk (Labscientific, M0841). Monoclonal antibodies used were Nanog (Cell Signaling, D73G4), CD133 (Cell Signaling, D2V8Q), CD44 (Cell Signaling, 8E2), ALDH1A1 (Cell Signaling, D9J7R), MDR1/ABCB1 (Cell Signaling, E1Y7B), HIF1-alpha (Cell Signaling, D5F3M), ABCG2 (Cell Signaling, D5V2K), EpCAM (Cell Signaling, VU1D9), EPAS-1 (Santa Cruz, 190B), CXCR-4 (Santa Cruz, 4G10), A20/TNFATP3 (Cell Signaling, D13H3), Vimentin (Invitrogen, MA5-11883), and GAPDH (HRP-60004, Proteintech), EGF Receptor (Cell Signaling, D38B1), Nanog (Cell Signaling, D73G4), E-Cadherin (Cell Signaling, 24E10), YAP (Santa Cruz, H-9). Target proteins were visualized with IgG secondary mouse or rabbit antibodies, and a chemiluminescent substrate (Santa Cruz, sc-2048).

#### **4.2.5 Drug pumping**

Cells seeded into the center reservoir of the flower microchannel device contains 6 satellite chambers: 3 connected by 5 $\mu$ m by 5 $\mu$ m channels, and 3 connected by 15 $\mu$ m by 15  $\mu$ m channels.  $20 \times 10^3$  cells were seeded at each of 6 satellite chambers and cells were allowed to migrate for ~ 7 days. At day 7, all devices were incubated with 0.01 (17 $\mu$ M) concentration of Doxorubicin for 4 hours. At 4 hours, devices had media replaced by imaging media, and cells were imaged by way of Doxorubicin autofluorescence by fluorescence microscopy. Following acquisition of images, devices were returned to 37<sup>0</sup> incubation overnight (~16 additional hours). After which, samples were re-imaged to determine % remaining intracellular Doxorubicin. The procedure was repeated for Doxorubicin concentrations, 2 $\mu$ M (4, 24, and 48 hrs), and 500 nM (4, and 24 hrs). Intercellular Doxorubicin concentrations were quantified using ImageJ.

#### **4.2.6 Cell viability after drug treatment**

Green Live/Dead Stain (ImmunoChemistry, 15J66) was used to measure cell viability following drug treatment. The working solution was prepared in PBS at a 1 :1000 ratio (v/v). Sample media was replaced by this mixture, and cells were incubated for 10 minutes. Substrate fluorescence was detected at 495 nm by fluorescence microscopy.

Breast cancer drugs were also treated with 5-Fluorouracil and Cisplatin, two clinically relevant anticancer drugs. Cells were treated with IC<sub>50</sub> concentrations of 25  $\mu$ M and 100  $\mu$ M respectively for 72 hours. At the end of incubation, samples were treated with Green PI, live cell-impermeable assay for detection of the percentage of live cells/dead cells.

#### **4.2.7 Migrated cells re-seeded**

6-well plates (n=3) containing microchannel devices were coated with collagen type I (Corning, REF 354236) overnight, then rinsed three times for neutralization.  $100 \times 10^3$  MDA-MB-231 breast cancer cells

were seeded into each well and cultured in 10% serum supplemented media for 7 days to allow for ample cell migration through microchannels. Cells were then collected, maintaining separation between 2D cells and migrated cells. 2D cells were lysed for western blot analysis, while migrated cells were re-seeded in the 2D culture environment and collected for analysis at the following time points: 2 days, 3 days, 4 days, and 8 days. Collected cell samples were lysed and prepared for western blot analysis.

### 4.3 Results

#### 4.3.1 CSC related biomarkers expression by migrated cells

Cluster of differentiation glycoprotein, CD44 expression decreased significantly in migrating cells as compared to nonmigrating cells, while CD133 expression increased significantly in migrating cells in comparison to nonmigrating cells, Figure 4.1. Identical patterns for the two stem cell markers was seen in MCF7 migrating cells, Figure 4.2.

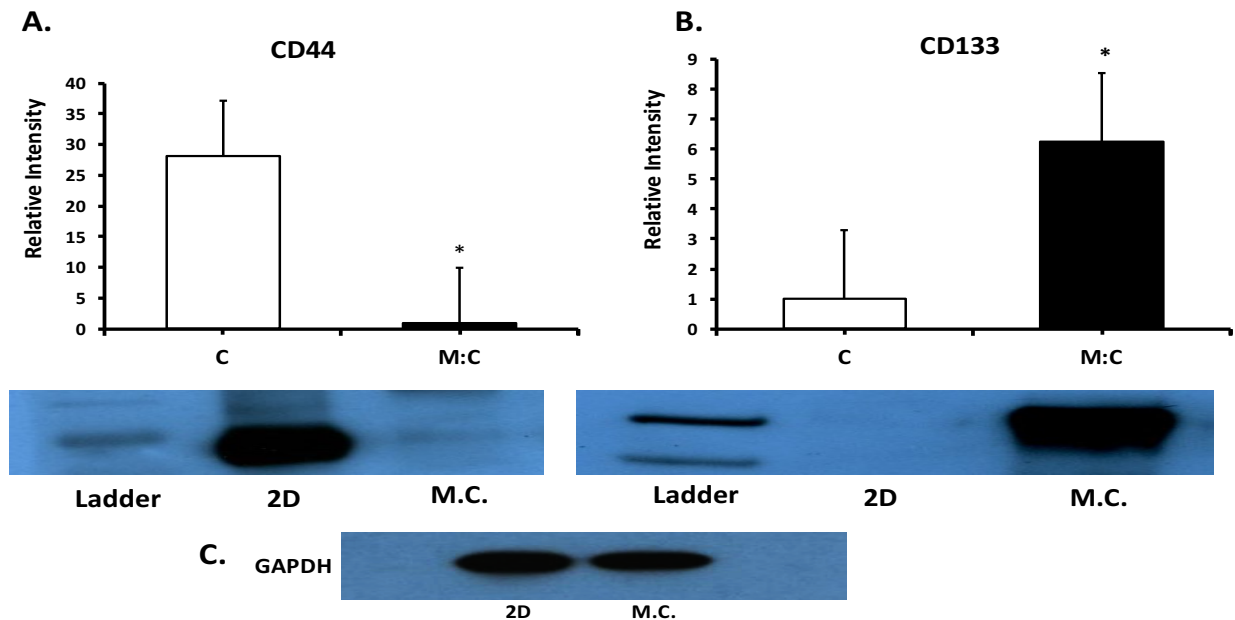


**Figure 4.1 MDA-MB-231 Breast cancer stem cell markers.** Expression differences in stem cell markers, CD44 (A) and CD133 (B) in MDA-MB-231 highly invasive breast cancer cell line. GAPDH is the loading control (C). \*  $P$ -value  $\leq 0.05$  when compared to 2D.

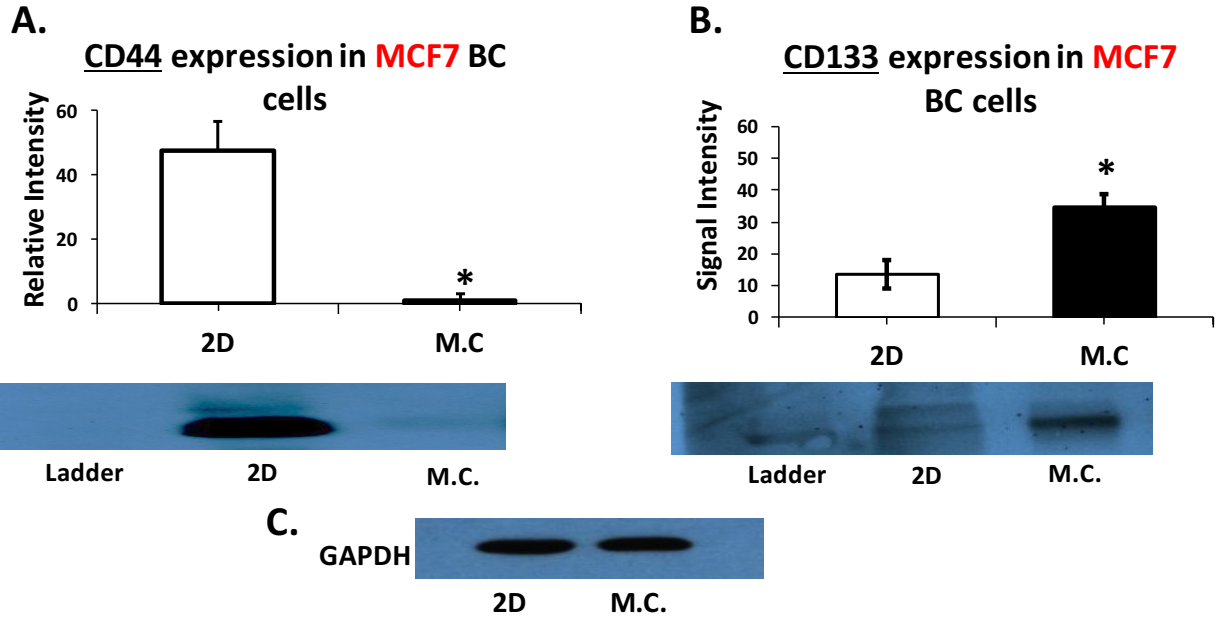


**Figure 4.2. MCF7 Breast cancer stem cell markers.** Expression differences in stem cell markers, CD44 (A) and CD133 (B) in MCF7 highly non-aggressive breast cancer cell line. GAPDH is the loading control (C). \*  $P$ -value  $\leq 0.05$  when compared to 2D.

### 4.3.2 Immunostaining of CSC and EMT markers

Increased expression of stem cell marker, CD133 was confirmed by immunostaining of breast cancer cells as they migrated through the microchannels, Figure 4.3. Interestingly, the increase in expression was more prominently visualized upon exit from the microchannels.

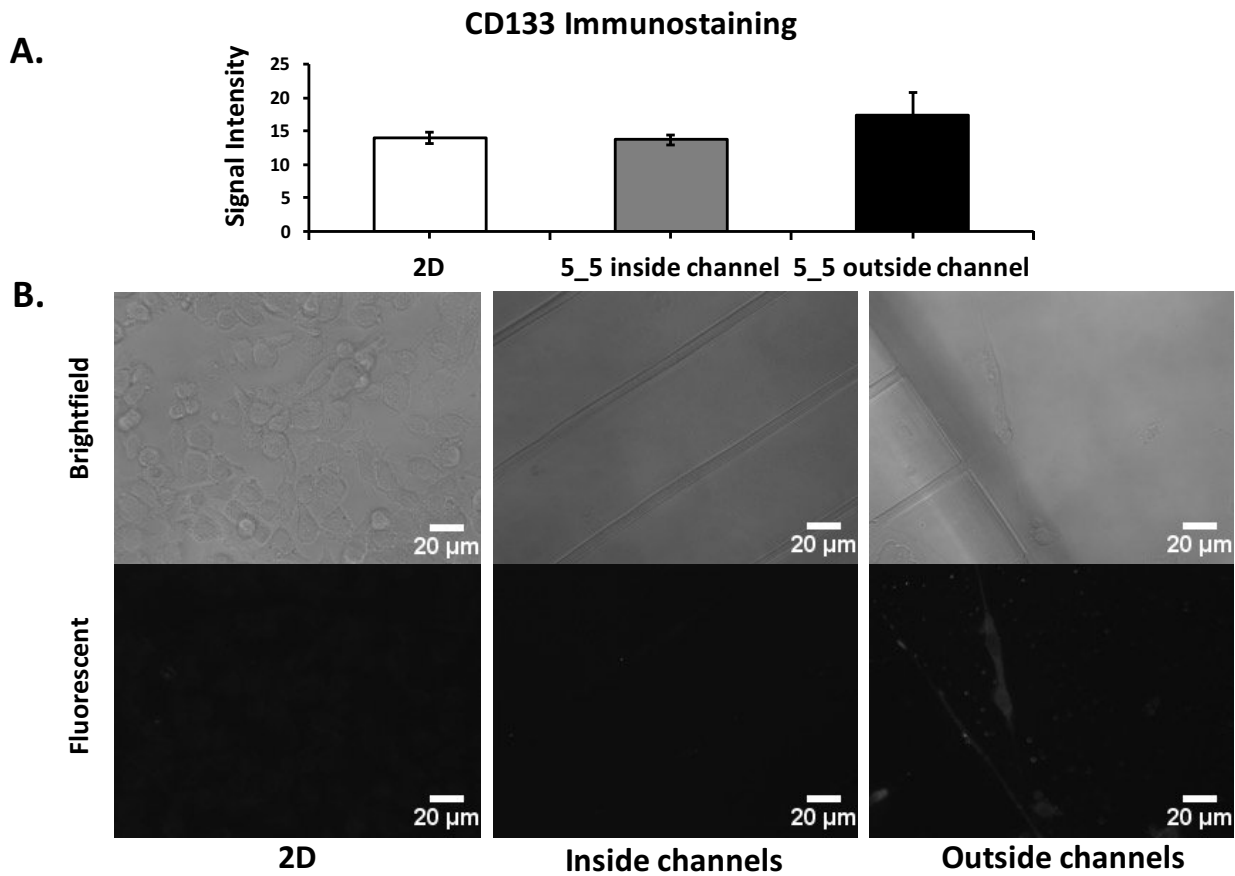


**Figure 4.3. Stem cell marker expression before, during, and after migration.** Immunostaining of breast cancer cells for expression of CD133 at three different time-points of migration. Quantification of fluorescent signal (A), and images showing fluorescent signals.

Staining of samples with a hypoxia/oxidative stress kit revealed that breast cancer cells which were grown in the 2D environment were under significantly more oxidative stress than cells which migrated through the microchannels, Figure 4.4.

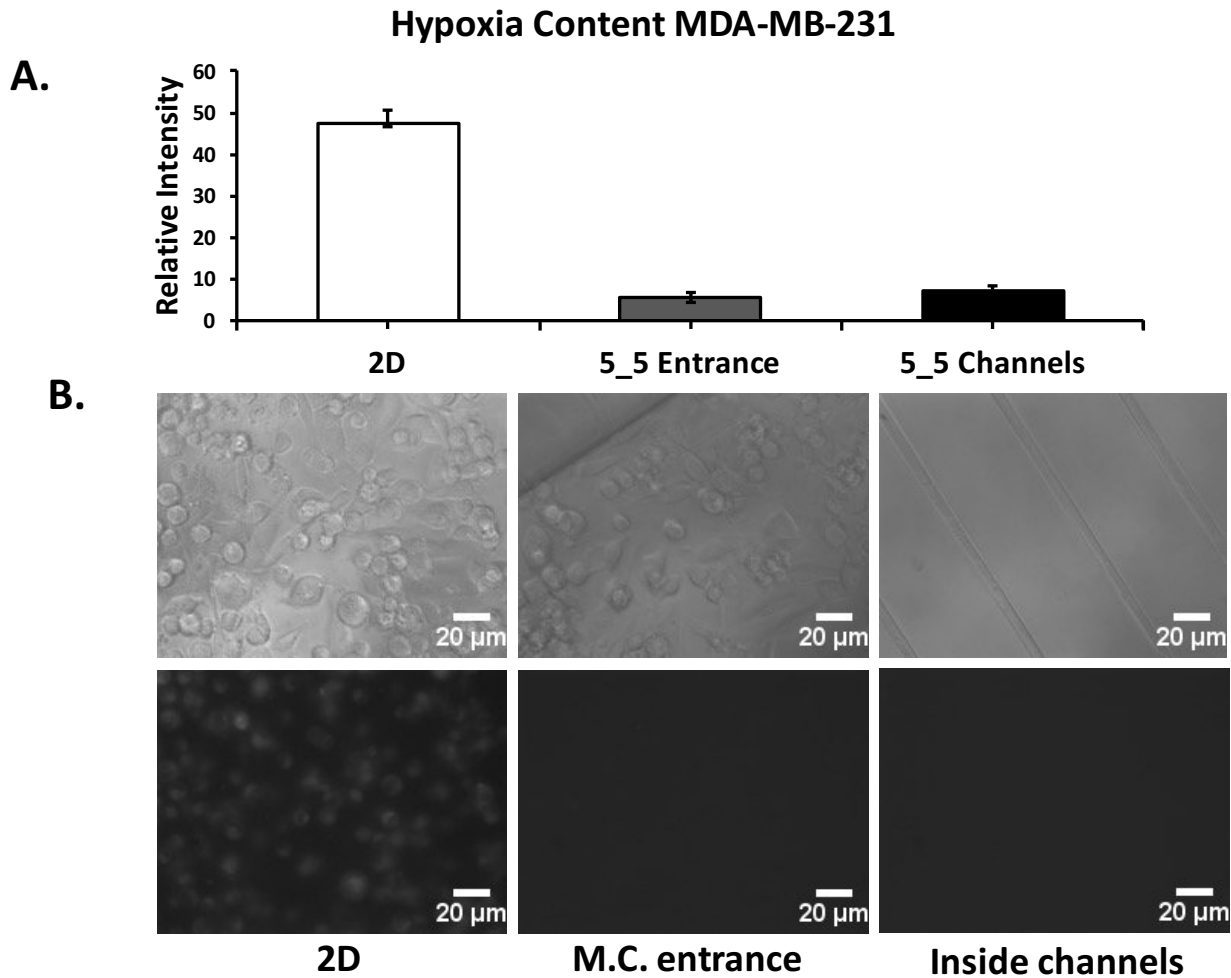


**Figure 4.4. Hypoxia/oxidative stress fluorescence signals of non-migrated cells vs. cells entering channels and those inside channels.** Hypoxia fluorescence signals of breast cancer cells for determination of oxidative stress of breast cancer cells in 2D vs. migrating cells. Quantification of fluorescent signal (A), and images showing fluorescent signals.

Immunostaining breast cancer samples with Yes-associated protein antibody uncovered a trend of higher cytoplasmic expression levels of the protein in cells in 2D, while cells that migrated expressed more concentrated levels inside the nucleus, Figure 4.5.

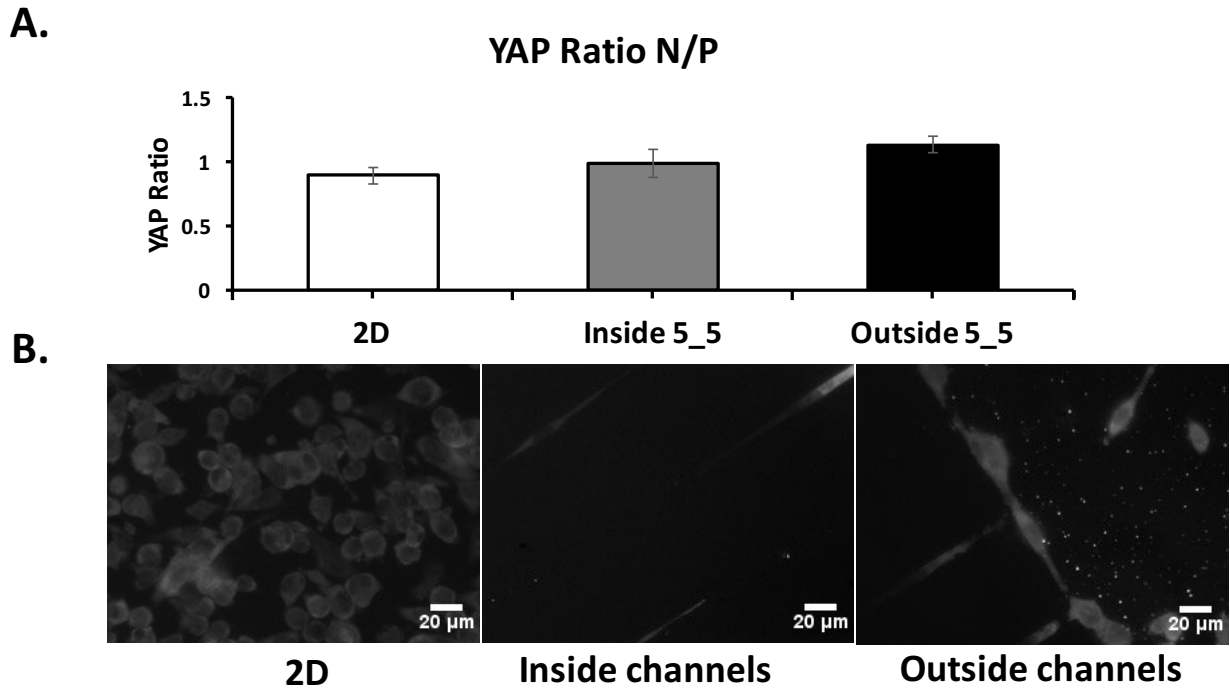


**Figure 4.5.** Yes-associated protein (YAP) expression differences in breast cancer cells. Aggressive breast cancer cells, MDA-MB-231 expressed more YAP in the cytoplasm before migration, and more in the nucleus during and after migration. Quantification of expression during three time-points (A), and fluorescence images (B) at same time-points.

### 4.3.3 Highly regulated chemotherapy resistance for migrating cells expressing membrane drug efflux pumps

Breast cancer cells were treated with 17  $\mu\text{M}$  of Dox anticancer drug, then allowed to incubate for 4 hour and 24-hour timepoints. Samples were imaged at both timepoints and subcellular compartmental (nuclear, cytoplasmic, and total cell) Dox autofluorescence was measured. Quantification revealed a significant decrease in nuclear and total cell Dox autofluorescence between 2D cells and cells which migrated through the 5\_5 microchannels, between 4 and 24-hour timepoints, Figure 4.6. In addition, two major breast cancer

associated drug efflux membrane glycoprotein, ABCG2 increased in expression in migrating cells compared to non-migrating cells.

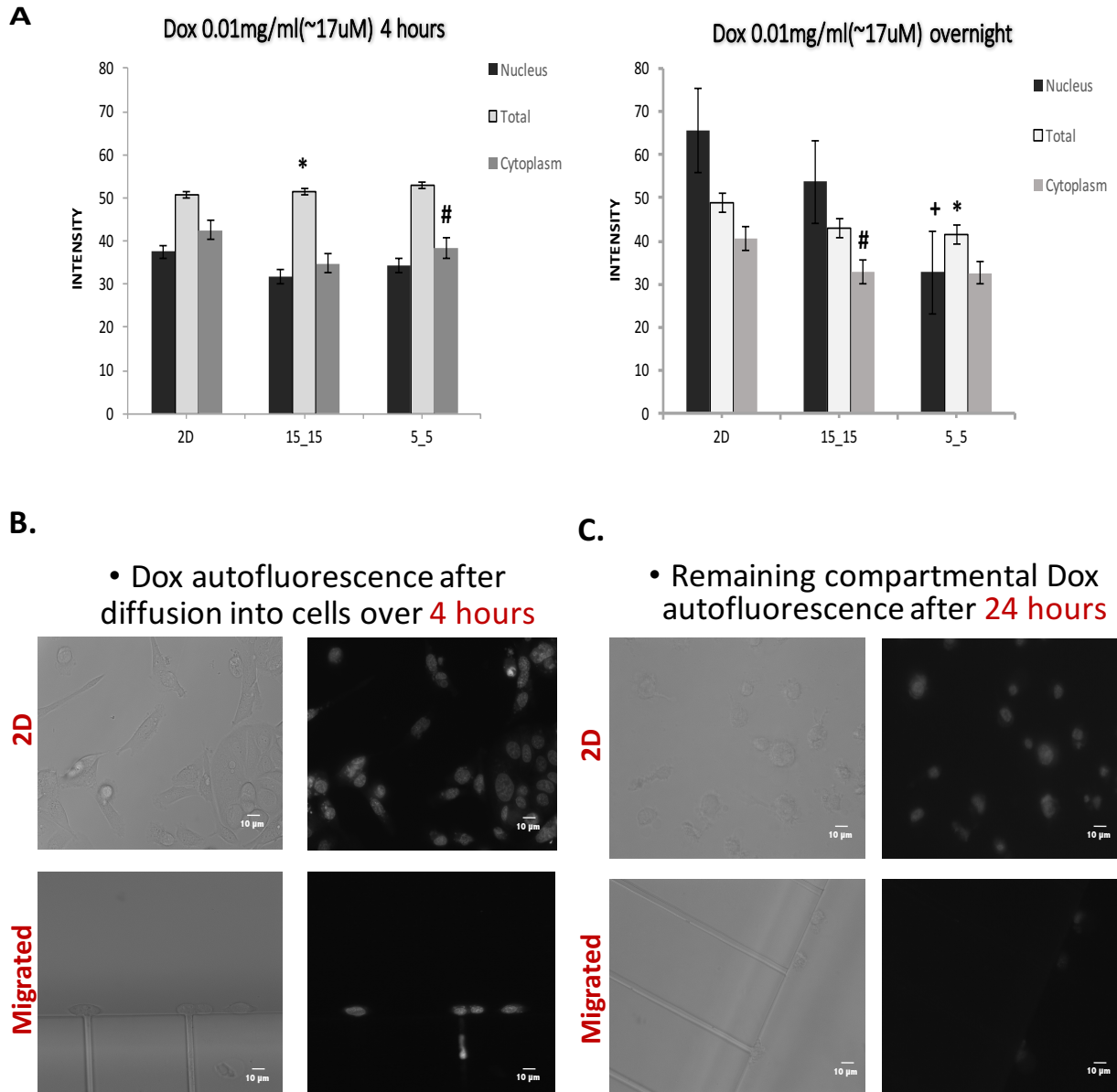
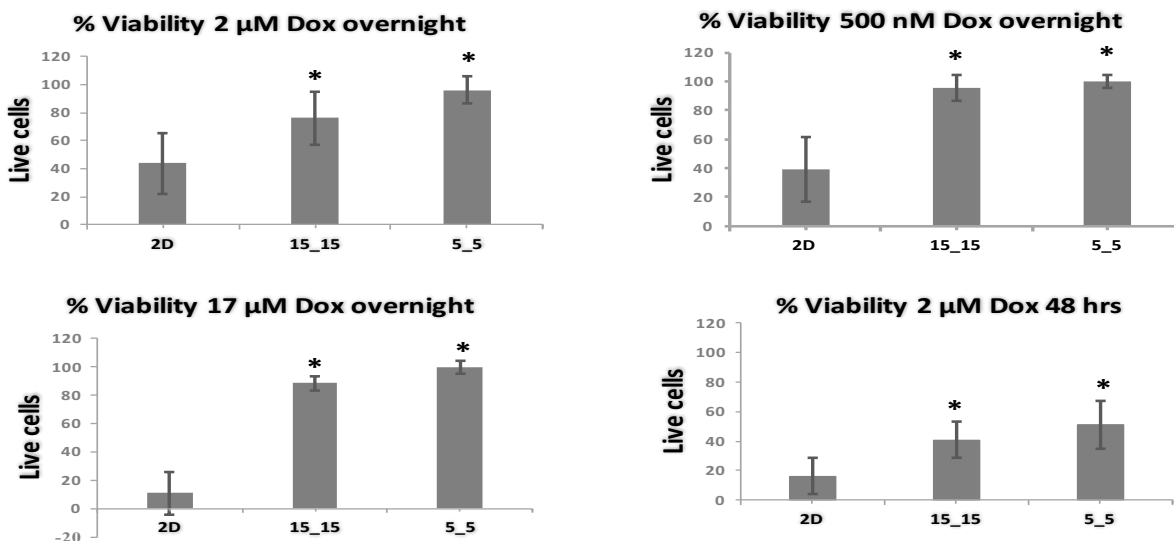


**Figure 4.6. Dox pumping from nucleus, then out of the cell over 24-hour period.** Breast cancer cells significantly decreased dox autofluorescence from the nucleus to the cytoplasm in cells in both 2D and migration over a 24-hour period (A). This difference in autofluorescence was much more significant in migrating cells (B). “+” =  $p$ -value  $\leq 0.05$  in comparison to 2D for “Nucleus”. “\*” =  $p$ -value  $\leq 0.05$  in comparison to 2D for “Whole cell”. “#” =  $p$ -value  $\leq 0.05$  in comparison to 2D for “Cytoplasm”.



Concurrent with the decrease in subcellular compartmental Dox fluorescence in breast cancer cells between 4 and 24-hour timepoints, we were able to visualize an overall decrease in Dox fluorescence in both 2D and migrated cells overtime Figure 4.6, with a more pronounced decrease in migrated cells. By utilizing a green fluorescent dye which fails to penetrate live cells, we were able to quantify percent viability of breast cancer cells following overnight Dox treatments of 500 nM, 2  $\mu$ M, & 17  $\mu$ M concentrations, as well as a 48-hour treatment at a 2  $\mu$ M concentration, Figure 4.7. The result was a consistent pattern of significant increase from <50% viable cells in the 2D environment to ~100% viability in migrated cells. A similar trend was seen for prostate cancer cell line, PC3 Figure 4.8.

**A.**



**B.**

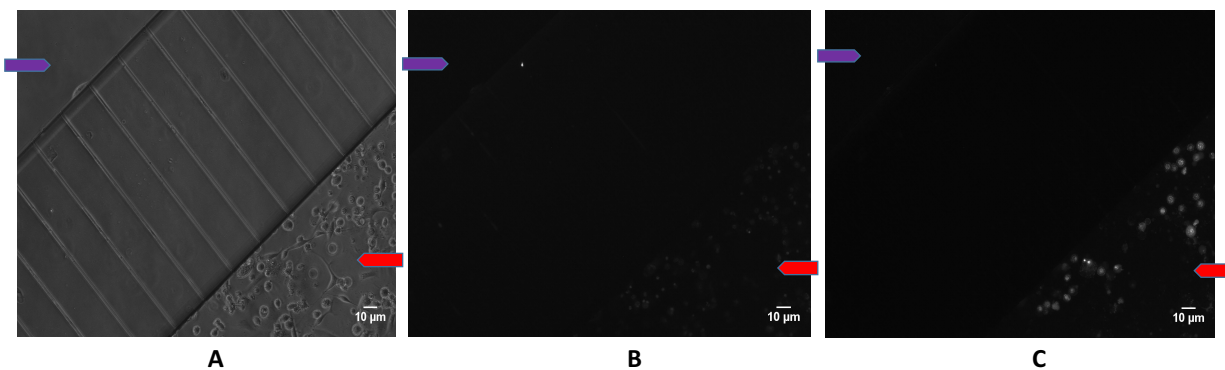


**Figure 4.7. % Viability in breast cancer cells after dox treatment.** MDA-MB-231 breast cancer cells displayed almost 100% viability after migration after incubation with multiple dox concentrations in comparison to relatively low viability percentages in non-migrating cells for the same concentrations (A). Purple arrowheads = channel exit, red arrowheads = 2D compartments. Dox fluorescence in 2D and microchannels (B-B) indicate dox diffusion into cells in both conditions. Green PI fluorescence in only 2D cells (B-C) indicate that dox only killed 2D cells. \* =  $p$ -value  $\leq 0.05$  in comparison to 2D.

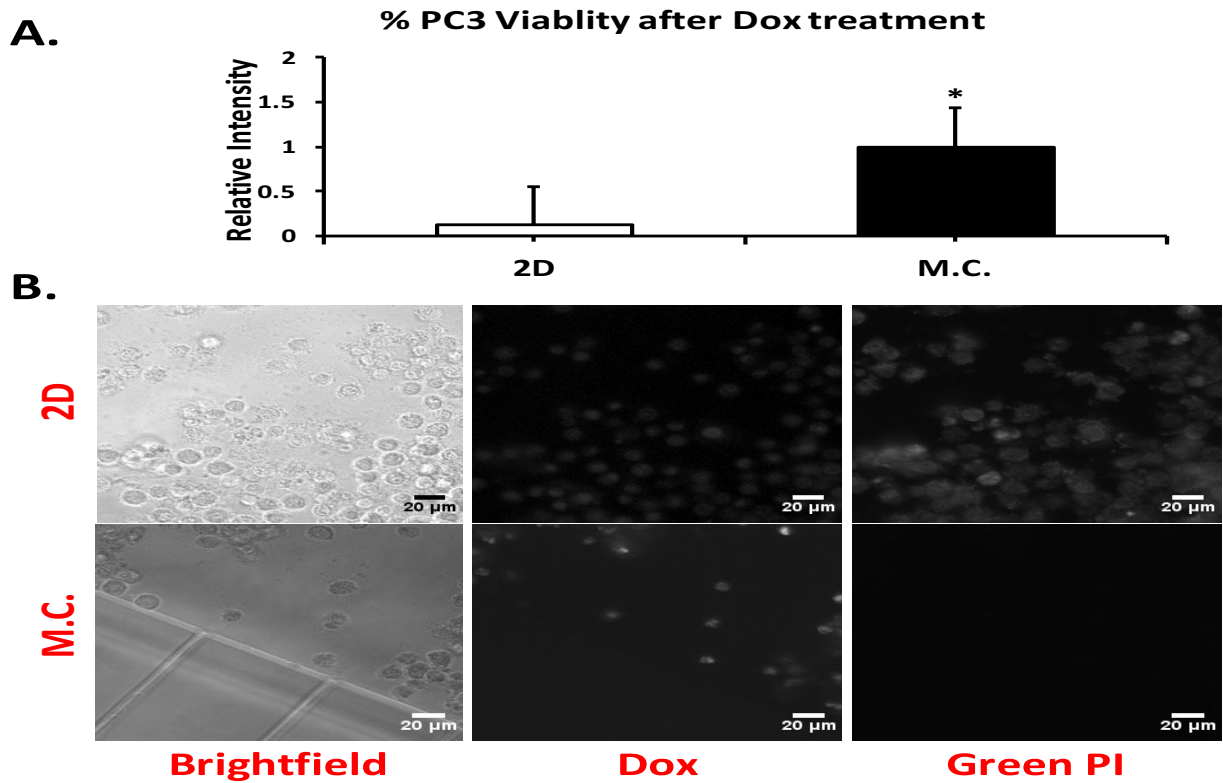


**Figure 4.8. % Viability in prostate cancer cells after dox treatment.** PC3 prostate cancer cells displayed almost 100% viability after migration following incubation with 17 $\mu$ M dox concentration, in comparison to < 20% viability of non-migrating cells for the same concentration (A). Brightfield and fluorescent images showing Dox-containing cells in 2D and M.C.s. Green PI fluorescence in only 2D cells (B) indicate that dox only killed 2D cells. \* =  $p$ -value  $\leq 0.05$  in comparison to 2D.

After treatment with Cisplatin, through there were 100% viable cells that migrated through the microchannels, it was not a significantly different number of viable cells than those in the 2D condition.

However, cells treated with 5-Fluorouracil died significantly leaving little more than 40% of living cells in the 2D condition, in comparison to the ~100% of viable migrated cells remaining, Figure 4.9.

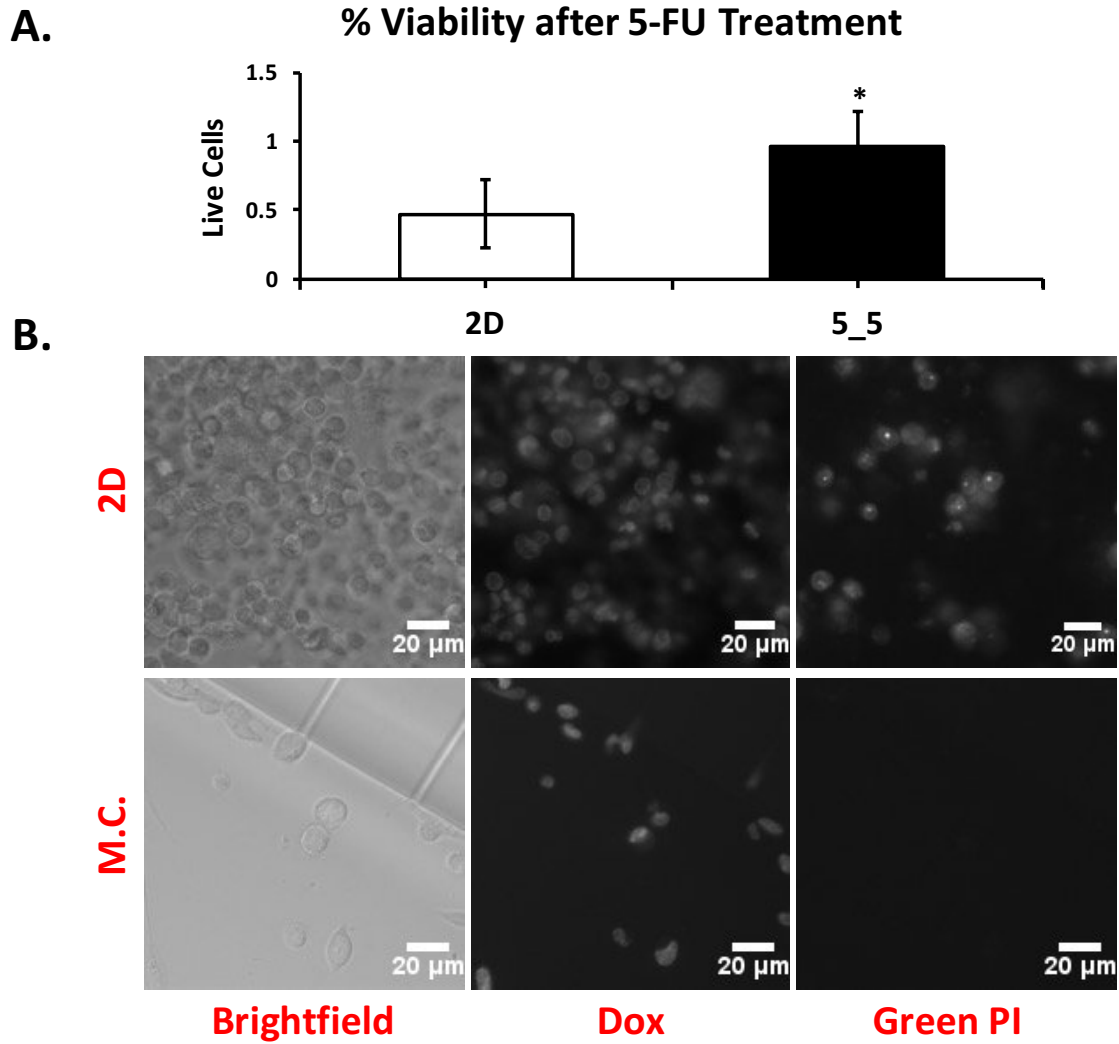


**Figure 4.9. Viability in prostate cancer cells after dox treatment.** PC3 prostate cancer cells displayed ~100% viability after migration after incubation with 17 $\mu$  dox concentration in comparison to relatively low viability percentages in non-migrating cells (A). Green PI fluorescence in only 2D cells (B) indicate that dox only killed 2D cells. \* =  $p$ -value  $\leq 0.05$  in comparison to 2D.

## **4.4 Discussion**

### **4.4.1 Stem cell markers**

As previously mentioned, stem cell markers; EpCAM, ALDH1A1, and Nanog all increased in expression when cells migrated through the microchannels. In addition to these markers, cluster of differentiation glycoproteins, CD44 and CD133 showed differential expressions in migrating cells. CD44 mediates cell-cell and cell-matrix interactions. Increased expression of the protein has been reported to be associated with the inflammatory response. Cancer studies have demonstrated the protein's ominous links to various downstream CSC and EMT transcription cascades. To a larger degree, it is believed that CD44<sup>high</sup>/CD24<sup>low</sup> breast cancer cells have definitively acquired tumorigenicity and self-renewal properties, endowing them with increased invasive and treatment evading capabilities. Consequently, we expected to see increased expression in migrating breast cancer cells. Nonetheless, the result was the opposite. Interestingly, prostate cancer migration studies have revealed a divergent role the protein seems to play in metastatic disease, establishing it as a tumor-suppressor that is able to block metastasis. In prostate cancer, its down-regulation has been coupled to metastatic stage. Based on the observed decrease in expression in migrating breast cancer cells, it is more probable that this is in fact also the mechanism of action for the protein in our experiment. Transmembrane glycoprotein CD133 is a foremost marker used to isolate stem cells of various tissues, including CSCs. As expected its expression was increased in migrating breast cancer cells, indicating likely acquisition of stem-like epigenetic features resulting from migration through 3D confinement. Similar trends were seen in expression patterns of CD133 and CD44 in MDA-MB-231 aggressive breast cancer cell line were seen in MCF7 non-aggressive breast cancer cell line.

#### 4.4.2 Dox viability and drug pumping

Initial 17  $\mu\text{M}$  concentration Dox treatment of breast cancer cells was practical for visualization of intracellular drug mobility, due to the degree of Dox autofluorescence at this concentration. Quantification of subcellular Dox fluctuation revealed a pattern of decrease in Dox fluorescence in migrated cells, from 4-hour to 24 hour incubation in both the nucleus and cell the as a whole. In contrast, Dox fluorescence increased significantly in the nucleus of 2D cells over the same span of time. Due to increased expression of two breast cancer multidrug resistance receptors in migrating cells, we deduce that there is a likely correlation between the magnitude of fluorescence decrease, and the up-regulation of drug flux receptors in migrated cells. Similarly, the observed decrease in Dox fluorescence presumably correlates with the substantially higher percent viability ( $> 90\%$ ) for migrated cancer cells, in comparison to percent viability ( $< 50\%$ ) for 2D cells. These results followed overnight treatment of cells in both conditions with 17  $\mu\text{M}$  and more clinically relevant, 2  $\mu\text{M}$  and 500 nM concentrations. A similar trend was observed for cells treated with 2  $\mu\text{M}$  Dox after 48 hours, decreasing further to ( $< 20\%$ ) and ( $< 60\%$ ) for 2D and migrated cells respectively. Since DNA is the target for the drug's mode of action, it makes sense that an increase in intranuclear drug concentration would result in decreased cell viability. Likewise, it is plausible that increased expression of drug transporters, whose main function is to metabolize or move toxins out of the cell, would be associated with diminished intracellular density of drug over time.

To determine if we would see the same trend of low vs high viability in 2D vs migrating cells respectively, we treated breast cancer cells with 5-Fluorouracil (5-FU), a clinically relevant breast cancer drug and metabolite which works by incorporating itself into DNA and RNA strands, thereby stimulating apoptosis. Utilizing the drug's  $\text{IC}_{50}$ , we found that  $\sim 40$  percent of cells in 2D survived the 72-hour treatment vs 100 percent survival of cells that had migrated. This is significant in that it suggests the 3D physical confinement of the microchannels is likely inducing an epigenetic change or series of changes, which are working together to protect these migrating cells from treatment associated cell death. It has been speculated that a

major contributing factor to 5-FU resistance in breast cancer is up-regulation of the enzyme, thymidylate synthase (TS).(104) TS is responsible for catalysis of the conversion of deoxyuridine monophosphate to deoxythymidine monophosphate. 5-FU inhibits this enzyme, causing DNA damage. Reports have shown that cancer cells which become resistant to this drug have up-regulated production of this enzyme. We suspect that this is a primary mechanism migrating cells in this experiment are utilizing to evade apoptosis during migration. Bearing this in mind, we are currently conducting an experiment to probe for TS expression levels in cells between the two conditions. Similarly, we will probe for expression levels of glutathione S-transferase (GST), an enzyme known to deactivate and metabolize toxic substances from cancer cells and release the toxic substance through lysozymes, in an attempt to detoxify the cells. This mechanism would explain the ability of these cancer cells to internalize a chemotherapeutic drug and be completely unaffected by it. We suspect this as another possible mechanism breast cancer cells in this experiment are taking advantage of.

#### **4.4.3 Hypoxia**

We previously demonstrated an increase in HIF1- $\alpha$  expression in migrating cells. HIF1- $\alpha$  is a transcription factor which mediates the cell's response to hypoxic conditions, being up-regulated in hypoxic conditions and degraded during normoxic conditions. The protein also has oxygen-independent functions which include regulating survival and proliferation of tumor cells upon aberrant activation. HIF1- $\alpha$  was upregulated 4-fold in migrating cells. So, we were interested to know which function was being activated during this migration. To do so, we used a hypoxia/oxidative stress dye which takes advantage of the nitroreductase activity present in hypoxic cells by converting the Nitro group to hydroxylamine (NHOH) and amino (NH<sub>2</sub>), releasing the fluorescent probe. As can be seen in cells which grew in 2D radiated significantly more fluorescence than did cells that migrated through the channels. This would lead to two possible conclusions, 1) conditions within the microchannels are normoxic in comparison



to those in 2D, 2) since migrating/migrated cells are not under oxidative stress, it is more likely that upregulation of HIF1- $\alpha$  in these cells has more to do with EMT than it does hypoxia.

#### **4.4.4 YAP protein expression**

The Yes-associated protein, otherwise known as YAP, is a 14-3-3 binding molecule that was originally recognized by virtue of its ability to bind to the SH3 domain of Yes. The highly conserved and ubiquitously expressed 14-3-3 proteins regulate differentiation, cell cycle progression and apoptosis by binding intracellular phosphoproteins involved in signal transduction.(105) YAP may link events at the plasma membrane and cytoskeleton to inhibition of transcription in the nucleus in a manner regulated by 14-3-3 proteins.(106) YAP is an oncoprotein located in the cytoplasm in an inactive form, and when activated, it translocates to the nucleus and activates the transcription of genes responsible for cell division and apoptosis.(107) YAP is one of the downstream regulatory proteins in the Hippo signaling pathway, which is important in cell proliferation, regeneration, organ development, and stem cell self-renewal. One of the cancer associated mechanisms of action of YAP protein is said to be by inhibition of the tumor suppressor, PTEN.(108) When the level of activated YAP is increased, the level of PTEN decreases. When YAP is phosphorylated and inhibited, PTEN function is restored and oncogene transcription is inhibited.(108) Accordingly, its plausible to surmise that migrating cells would increase expression of the protein during and after cell migration, in comparison to 2D cells. This in fact was the case with breast cancer cells. It was a gradual increase, but evident nonetheless. As can be seen in cells began to express higher concentrations of the protein in the nucleus during and after migration than did cells that had not migrated. What can be presumed from this data is that during migration, YAP is being activated and subsequently taken into the cell nucleus. After which, tumor suppression is being inhibited while oncogenes are being transcribed. Oncogene activation which results in cell division, inhibition of apoptosis, stem cell self-renewal, or all foregoing.

In conclusion, we have uncovered a range of epigenetic changes which signify the likelihood of cancer cells undergoing neoplasticity resulting in dedifferentiation while migrating in a 3D confined space. EMT activities have been demonstrated in cancer progression many times over. Because EMT shares many of the downstream pathways as do regulatory genes for induction and maintenance of stemness, it is certainly conceivable that the two work together to endow epithelial tumor cells with the mesenchymal features they need to escape from the primary tumor and survive the long journey to distant sites for repopulation and development of secondary tumors. The CSC Theory is one that has been controversial for many years. However, it is becoming increasingly backed by evidence which is causing the scientific community to re-evaluate its need for design of new anticancer treatments.

## References

1. Desantis CE, Fedewa SA, Sauer AG, Kramer JL, Smith RA, Jemal A. Breast Cancer Statistics , 2015 : Convergence of Incidence Rates Between Black and White Women. *A cancer J Clin*. 2016;66(1):31–42.
2. Siegel RL, Miller KD, Jemal A. Cancer statistics, 2018. *CA Cancer J Clin* [Internet]. 2018;68(1):7–30. Available from: <http://doi.wiley.com/10.3322/caac.21442>
3. Siegel RL, Miller KD, Jemal A. Cancer statistics. *CA Cancer J Clin*. 2016;66(1):7–30.
4. Miller KD, Siegel RL, Lin CC, Mariotto AB, Kramer JL, Rowland JH, et al. Cancer treatment and survivorship statistics, 2016. *CA Cancer J Clin* [Internet]. 2016;66(4):271–89. Available from: <http://doi.wiley.com/10.3322/caac.21349>
5. Dawood S. Triple-Negative Breast Cancer. *Drugs*. 2010;70(17):2247–58.
6. Lehmann BD, Shyr Y, Pietenpol JA, Lehmann BD, Bauer JA, Chen X, et al. Identification of human triple-negative breast cancer subtypes and preclinical models for selection of targeted therapies Find the latest version : Identification of human triple-negative breast cancer subtypes and preclinical models for selection of targ. 2011;121(7):2750–67.
7. Liedtke C, Mazouni C, Hess KR, André F, Tordai A, Mejia JA, et al. Response to neoadjuvant therapy and long-term survival in patients with triple-negative breast cancer. *J Clin Oncol*. 2008;26(8):1275–81.
8. Burstein MD, Tsimelzon A, Poage GM, Covington KR, Contreras A, Fuqua SAW, et al. Comprehensive genomic analysis identifies novel subtypes and targets of triple-negative breast cancer. *Clin Cancer Res*. 2015;21(7):1688–98.
9. Criscitiello C, Azim HA, Schouten PC, Linn SC, Sotiriou C. Understanding the biology of triple-negative breast cancer. *Ann Oncol*. 2012;23(SUPPL. 6).

10. Dent SF. The role of VEGF in triple-negative breast cancer: Where do we go from here? *Ann Oncol.* 2009;20(10):1615–7.
11. He J, Peng R, Yuan Z, Wang S, Peng J, Lin G, et al. Prognostic value of androgen receptor expression in operable triple-negative breast cancer: A retrospective analysis based on a tissue microarray. *Med Oncol.* 2012;29(2):406–10.
12. Zhao S, Ma W, Zhang M, Tang D, Shi Q, Xu S, et al. High expression of CD147 and MMP-9 is correlated with poor prognosis of triple-negative breast cancer (TNBC) patients. *Med Oncol.* 2013;30(1).
13. Langley RR, Fidler IJ. The seed and soil hypothesis revisited-The role of tumor-stroma interactions in metastasis to different organs. *Int J Cancer.* 2011;128(11):2527–35.
14. Pienta KJ, Robertson BA, Coffey DS, Taichman RS. The cancer diaspora: Metastasis beyond the seed and soil hypothesis. *Clin Cancer Res.* 2013;19(21):5849–55.
15. Hart IR. “Seed and soil” revisited: mechanisms of site-specific metastasis. *Cancer Metastasis Rev.* 1982;1(1):5–16.
16. Wicha MS. Cancer stem cells and metastasis: Lethal seeds. *Clin Cancer Res.* 2006;12(19):5606–7.
17. Kalluri R. EMT : When epithelial cells decide to become Find the latest version : Review series introduction EMT : When epithelial cells decide to become mesenchymal-like cells. 2009;119(6):1417–9.
18. Sarrió D, Rodríguez-Pinilla SM, Hardisson D, Cano A, Moreno-Bueno G, Palacios J. Epithelial-mesenchymal transition in breast cancer relates to the basal-like phenotype. *Cancer Res.* 2008;68(4):989–97.
19. Abraham BK, Fritz P, McClellan M, Hauptvogel P, Athellogou M, Brauch H. Prevalence of

- CD44+/CD24-/low cells in breast cancer may not be associated with clinical outcome but may favor distant metastasis. *Clin Cancer Res.* 2005;11:1154–9.
20. Aktas B, Tewes M, Fehm T, Hauch S, Kimmig R, Kasimir-Bauer S. Stem cell and epithelial-mesenchymal transition markers are frequently overexpressed in circulating tumor cells of metastatic breast cancer patients. *Breast Cancer Res.* 2009;11(4):1–9.
  21. De Laurentiis M, Cianniello D, Caputo R, Stanzione B, Arpino G, Cinieri S, et al. Treatment of triple negative breast cancer (TNBC): Current options and future perspectives. *Cancer Treat Rev* [Internet]. Elsevier Ltd; 2010;36(SUPPL. 3):S80–6. Available from: [http://dx.doi.org/10.1016/S0305-7372\(10\)70025-6](http://dx.doi.org/10.1016/S0305-7372(10)70025-6)
  22. Toft DJ, Cryns VL. Minireview: Basal-Like Breast Cancer: From Molecular Profiles to Targeted Therapies. *Mol Endocrinol* [Internet]. 2011;25(2):199–211. Available from: <https://academic.oup.com/mend/article-lookup/doi/10.1210/me.2010-0164>
  23. Lehmann BD, Jovanović B, Chen X, Estrada M V., Johnson KN, Shyr Y, et al. Refinement of Triple-Negative Breast Cancer Molecular Subtypes: Implications for Neoadjuvant Chemotherapy Selection. *PLoS One.* 2016;11(6):e0157368.
  24. Yu K Da, Zhu R, Zhan M, Rodriguez AA, Yang W, Wong S, et al. Identification of prognosis-relevant subgroups in patients with chemoresistant triple-negative breast cancer. *Clin Cancer Res.* 2013;19(10):2723–33.
  25. Sharma P, Allison JP. Immune checkpoint targeting in cancer therapy: Toward combination strategies with curative potential. *Cell* [Internet]. Elsevier Inc.; 2015;161(2):205–14. Available from: <http://dx.doi.org/10.1016/j.cell.2015.03.030>
  26. Meyer AAS, Miller MA, Gertler FB, Douglas A. Title : AXL Diversifies EGFR Signaling and Mitigates Response to EGFR- Targeted Therapeutics in Triple Negative Breast

- Carcinoma Cells. 2013;6(March).
27. Barton VN, D'Amato NC, Gordon MA, Lind HT, Spoelstra NS, Babbs BL, et al. Multiple Molecular Subtypes of Triple-Negative Breast Cancer Critically Rely on Androgen Receptor and Respond to Enzalutamide In Vivo. *Mol Cancer Ther* [Internet]. 2015;14(3):769–78. Available from: <http://mct.aacrjournals.org/cgi/doi/10.1158/1535-7163.MCT-14-0926>
  28. Anderson KN, Schwab RB, Martinez ME. Reproductive risk factors and breast cancer subtypes: A review of the literature. *Breast Cancer Res Treat*. 2014;144(1):1–10.
  29. Polyak K. Review series introduction Heterogeneity in breast cancer. *JClinInvest*. 2011;121(10):2011–3.
  30. Petrelli F, Coinu A, Borgonovo K, Cabiddu M, Ghilardi M, Lonati V, et al. The value of platinum agents as neoadjuvant chemotherapy in triple-negative breast cancers: A systematic review and meta-analysis. *Breast Cancer Res Treat*. 2014;144(2):223–32.
  31. Huber MA, Kraut N, Beug H. Molecular requirements for epithelial-mesenchymal transition during tumor progression. *Curr Opin Cell Biol*. 2005;17(5 SPEC. ISS.):548–58.
  32. Thompson E, Newgreen D. Carcinoma Invasion and Metastasis : A Role for Epithelial-Mesenchymal Transition ? *Cancer Res* [Internet]. 2005;65(14):5991–5. Available from: <http://cancerres.aacrjournals.org/content/65/14/5991.1.short>
  33. Mallini P, Lennard T, Kirby J, Meeson A. Epithelial-to-mesenchymal transition: What is the impact on breast cancer stem cells and drug resistance. *Cancer Treat Rev* [Internet]. Elsevier Ltd; 2014;40(3):341–8. Available from: <http://dx.doi.org/10.1016/j.ctrv.2013.09.008>
  34. Singh A, Settleman J. EMT, cancer stem cells and drug resistance: An emerging axis of evil

- in the war on cancer. *Oncogene* [Internet]. Nature Publishing Group; 2010;29(34):4741–51. Available from: <http://dx.doi.org/10.1038/onc.2010.215>
35. Kotiyal S, Bhattacharya S. Breast cancer stem cells, EMT and therapeutic targets. *Biochem Biophys Res Commun* [Internet]. Elsevier Inc.; 2014;453(1):112–6. Available from: <http://dx.doi.org/10.1016/j.bbrc.2014.09.069>
  36. Mimeault M, Batra SK. New advances on critical implications of tumor- and metastasis-initiating cells in cancer progression, treatment resistance and disease recurrence. *Histol Histopathol* [Internet]. 2010;25(8):1057–73. Available from: <http://www.ncbi.nlm.nih.gov/pubmed/20552555> <http://www.pubmedcentral.nih.gov/articlerender.fcgi?artid=PMC2997575>
  37. Thiery JP, Acloque H, Huang RYJ, Nieto MA. Epithelial-Mesenchymal Transitions in Development and Disease. *Cell*. 2009;139(5):871–90.
  38. Shook D, Keller R. Mechanisms, mechanics and function of epithelial-mesenchymal transitions in early development. *Mech Dev*. 2003;120(11):1351–83.
  39. Jeong H, Ryu YJ, An J, Lee Y, Kim A. Epithelial-mesenchymal transition in breast cancer correlates with high histological grade and triple-negative phenotype. *Histopathology*. 2012;60(6 B):87–95.
  40. Felipe Lima J, Nofech-Mozes S, Bayani J, Bartlett J. EMT in Breast Carcinoma—A Review. *J Clin Med* [Internet]. 2016;5(7):65. Available from: <http://www.mdpi.com/2077-0383/5/7/65>
  41. Doyle LA, Ross DD. Multidrug resistance mediated by the breast cancer resistance protein BCRP (ABCG2). *Oncogene*. 2003;22(47 REV. ISS. 6):7340–58.
  42. Fuxe J, Vincent T, De Herreros AG. Transcriptional crosstalk between TGF $\beta$  and stem cell

- pathways in tumor cell invasion: Role of EMT promoting Smad complexes. *Cell Cycle*. 2010;9(12):2363–74.
43. Kong X, Li G, Yuan Y, He Y, Wu X, Zhang W, et al. MicroRNA-7 inhibits epithelial-to-mesenchymal transition and metastasis of breast cancer cells via targeting FAK expression. *PLoS One*. 2012;7(8).
  44. Hawsawi Y, El-Gendy R, Twelves C, Speirs V, Beattie J. Insulin-like growth factor - Oestradiol crosstalk and mammary gland tumourigenesis. *Biochim Biophys Acta - Rev Cancer* [Internet]. Elsevier B.V.; 2013;1836(2):345–53. Available from: <http://dx.doi.org/10.1016/j.bbcan.2013.10.005>
  45. Wang Z, Li Y, Ahmad A, Azmi AS, Kong D, Banerjee S, et al. Targeting miRNAs involved in cancer stem cell and EMT regulation: An emerging concept in overcoming drug resistance. *Drug Resist Updat*. 2010;13(4–5):109–18.
  46. Sackmann EK, Fulton AL, Beebe DJ. The present and future role of microfluidics in biomedical research. *Nature* [Internet]. Nature Publishing Group; 2014;507(7491):181–9. Available from: <http://dx.doi.org/10.1038/nature13118>
  47. Andersson H, Van den Berg A. Microfluidic devices for cellomics: A review. *Sensors Actuators, B Chem*. 2003;92(3):315–25.
  48. Berthier E, Young EWK, Beebe D. Engineers are from PDMS-land, biologists are from polystyrenia. *Lab Chip*. 2012;12(7):1224–37.
  49. Brabletz T. To differentiate or not-routes towards metastasis. *Nat Rev Cancer* [Internet]. Nature Publishing Group; 2012;12(6):425–36. Available from: <http://dx.doi.org/10.1038/nrc3265>
  50. Martinez-Outschoorn UE, Pavlides S, Howell A, Pestell RG, Tanowitz HB, Sotgia F, et al.



- Stromal-epithelial metabolic coupling in cancer: Integrating autophagy and metabolism in the tumor microenvironment. *Int J Biochem Cell Biol.* 2011;43(7):1045–51.
51. Osta W. EpCAM Is Overexpressed in Breast Cancer and Is a Potential Target for Breast Cancer Gene Therapy. *Cancer Res.* 2004;64(16):5818–24.
  52. Wang D, Lu P, Zhang H, Luo M, Zhang X, Wei X, et al. Oct-4 and Nanog promote the epithelial-mesenchymal transition of breast cancer stem cells and are associated with poor prognosis in breast cancer patients. *Oncotarget* [Internet]. 2014;5(21):10803–15. Available from:  
<http://www.pubmedcentral.nih.gov/articlerender.fcgi?artid=4279411&tool=pmcentrez&rendertype=abstract>
  53. Zhang C, Samanta D, Lu H, Bullen JW, Zhang H, Chen I, et al. Hypoxia induces the breast cancer stem cell phenotype by HIF-dependent and ALKBH5-mediated m<sup>6</sup>A-demethylation of NANOG mRNA. *Proc Natl Acad Sci.* 2016;113(14):E2047–56.
  54. Han J, Zhang F, Yu M, Zhao P, Ji W, Zhang H, et al. RNA interference-mediated silencing of NANOG reduces cell proliferation and induces G0/G1 cell cycle arrest in breast cancer cells. *Cancer Lett.* Elsevier Ireland Ltd; 2012;321(1):80–8.
  55. Nagata T, Shimada Y, Sekine S, Hori R, Matsui K, Okumura T, et al. Prognostic significance of NANOG and KLF4 for breast cancer. *Breast Cancer.* 2014;21(1):96–101.
  56. Clark R, Kerr ID, Callaghan R. Multiple drugbinding sites on the R482G isoform of the ABCG2 transporter. *Br J Pharmacol.* 2006;149(5):506–15.
  57. Vendrell JA, Ghayad S, Ben-Larbi S, Dumontet C, Mechti N, Cohen PA. A20/TNFAIP3, a new estrogen-regulated gene that confers tamoxifen resistance in breast cancer cells. *Oncogene.* 2007;26(32):4656–67.

58. Zhang Z, Vuori K, Reed JC, Ruoslahti E. The alpha 5 beta 1 integrin supports survival of cells on fibronectin and up-regulates Bcl-2 expression. *Proc Natl Acad Sci* [Internet]. 1995;92(13):6161–5. Available from: <http://www.pnas.org/cgi/doi/10.1073/pnas.92.13.6161>
59. Torre LA, Bray F, Siegel RL, Ferlay J, Lortet-tieulent J, Jemal A. Global Cancer Statistics, 2012. *CA a cancer J Clin* [Internet]. 2015;65(2):87–108. Available from: <http://onlinelibrary.wiley.com/doi/10.3322/caac.21262/abstract>
60. Vracko R. Basal lamina scaffold-anatomy and significance for maintenance of orderly tissue structure. *Am J Pathol* [Internet]. 1974;77(2):314–46. Available from: <http://www.pubmedcentral.nih.gov/articlerender.fcgi?artid=1910920&tool=pmcentrez&rendertype=abstract>
61. Yurchenco PD, O’Rear JJ. Basal lamina assembly. *Curr Opin Cell Biol*. 1994;6(5):674–81.
62. Loessner D, Stok KS, Lutolf MP, Hutmacher DW, Clements JA, Rizzi SC. Bioengineered 3D platform to explore cell-ECM interactions and drug resistance of epithelial ovarian cancer cells. *Biomaterials* [Internet]. Elsevier Ltd; 2010;31(32):8494–506. Available from: <http://dx.doi.org/10.1016/j.biomaterials.2010.07.064>
63. Hartsock A, Nelson WJ. Adherens and tight junctions: Structure, function and connections to the actin cytoskeleton. *Biochim Biophys Acta - Biomembr*. 2008;1778(3):660–9.
64. Vuoriluoto K, Haugen H, Kiviluoto S, Mpindi JP, Nevo J, Gjerdrum C, et al. Vimentin regulates EMT induction by Slug and oncogenic H-Ras and migration by governing Axl expression in breast cancer. *Oncogene* [Internet]. Nature Publishing Group; 2011;30(12):1436–48. Available from: <http://dx.doi.org/10.1038/onc.2010.509>
65. Coley HM. Mechanisms and strategies to overcome chemotherapy resistance in metastatic

- breast cancer. *Cancer Treat Rev.* 2008;34(4):378–90.
66. Wilson C, Nicholes K, Bustos D, Lin E, Song Q, Stephan J-P, et al. Overcoming EMT-associated resistance to anti-cancer drugs via Src/FAK pathway inhibition. *Oncotarget* [Internet]. 2014;5(17). Available from: <http://www.oncotarget.com/fulltext/2397>
  67. P.S. Hodgkinson, A.C.Mackinnon PTS. Title: Extracellular matrix regulation of drug resistance in small-cell lung cancer. *Int J Radiat Biol.* 2007;83(11–12):733–41.
  68. Xu R, Boudreau A, Bissell MJ. Tissue architecture and function: Dynamic reciprocity via extra- and intra-cellular matrices. *Cancer Metastasis Rev.* 2009;28(1–2):167–76.
  69. Li ACY. Basement membrane components. *J Clin Pathol* [Internet]. 2003;56(12):885–7. Available from: <http://jcp.bmj.com/cgi/doi/10.1136/jcp.56.12.885>
  70. Rajan N, Habermehl J, Côté MF, Doillon CJ, Mantovani D. Preparation of ready-to-use, storable and reconstituted type I collagen from rat tail tendon for tissue engineering applications. *Nat Protoc.* 2007;1(6):2753–8.
  71. Foroni C, Broggin M, Generali D, Damia G. Epithelial-mesenchymal transition and breast cancer: Role, molecular mechanisms and clinical impact. *Cancer Treat Rev* [Internet]. Elsevier Ltd; 2012;38(6):689–97. Available from: <http://dx.doi.org/10.1016/j.ctrv.2011.11.001>
  72. Sulzmaier FJ, Jean C, Schlaepfer DD. FAK in cancer: Mechanistic findings and clinical applications. *Nat Rev Cancer* [Internet]. Nature Publishing Group; 2014;14(9):598–610. Available from: <http://dx.doi.org/10.1038/nrc3792>
  73. Gherardi E, Birchmeier W, Birchmeier C, Woude G Vande. Targeting MET in cancer: Rationale and progress. *Nat Rev Cancer.* 2012;12(2):89–103.
  74. Sakuma Y, Matsukuma S, Nakamura Y, Yoshihara M, Koizume S, Sekiguchi H, et al.

- Enhanced autophagy is required for survival in EGFR-independent EGFR-mutant lung adenocarcinoma cells. *Lab Invest* [Internet]. Nature Publishing Group; 2013;93(10):1137–46. Available from: <http://dx.doi.org/10.1038/labinvest.2013.102>
75. Rakha EA, Reis-Filho JS, Ellis IO. Basal-like breast cancer: A critical review. *J Clin Oncol*. 2008;26(15):2568–81.
  76. Lever E, Sheer D. The role of nuclear organization in cancer. *J Pathol*. 2010;220(September):114–25.
  77. Reis-Filho JS, Tutt ANJ. Triple negative tumours: A critical review. *Histopathology*. 2008;52(1):108–18.
  78. Pao W, Chmielecki J. Rational, biologically based treatment of EGFR-mutant non-small-cell lung cancer. *Nat Rev Cancer* [Internet]. Nature Publishing Group; 2010;10(11):760–74. Available from: <http://dx.doi.org/10.1038/nrc2947>
  79. Zhong X, Rescorla FJ. Cell surface adhesion molecules and adhesion-initiated signaling: Understanding of anoikis resistance mechanisms and therapeutic opportunities. *Cell Signal* [Internet]. Elsevier Inc.; 2012;24(2):393–401. Available from: <http://dx.doi.org/10.1016/j.cellsig.2011.10.005>
  80. Chiarugi P, Giannoni E. Anoikis: A necessary death program for anchorage-dependent cells. *Biochem Pharmacol*. 2008;76(11):1352–64.
  81. Horbinski C, Mojesky C, Kyprianou N. Live free or die: Tales of homeless (cells) in cancer. *Am J Pathol* [Internet]. American Society for Investigative Pathology; 2010;177(3):1044–52. Available from: <http://dx.doi.org/10.2353/ajpath.2010.091270>
  82. Zhang Y, Jain R, Zhu M. Recent Progress and Advances in HGF/MET-Targeted Therapeutic Agents for Cancer Treatment. *Biomedicines* [Internet]. 2015;3(1):149–81.

Available from: <http://www.mdpi.com/2227-9059/3/1/149/>

83. Jong BK. Three-dimensional tissue culture models in cancer biology. *Semin Cancer Biol.* 2005;15(5 SPEC. ISS.):365–77.
84. Weigelt B, Ghajar CM, Bissell MJ. The need for complex 3D culture models to unravel novel pathways and identify accurate biomarkers in breast cancer. *Adv Drug Deliv Rev* [Internet]. Elsevier B.V.; 2014;69–70:42–51. Available from: <http://dx.doi.org/10.1016/j.addr.2014.01.001>
85. Szot CS, Buchanan CF, Freeman JW, Rylander MN. 3D in vitro bioengineered tumors based on collagen I hydrogels. *Biomaterials* [Internet]. Elsevier Ltd; 2011;32(31):7905–12. Available from: <http://dx.doi.org/10.1016/j.biomaterials.2011.07.001>
86. Page H, Flood P, Reynaud EG. Three-dimensional tissue cultures: Current trends and beyond. *Cell Tissue Res.* 2013;352(1):123–31.
87. Armentano I, Dottori M, Fortunati E, Mattioli S, Kenny JM. Biodegradable polymer matrix nanocomposites for tissue engineering: A review. *Polym Degrad Stab* [Internet]. Elsevier Ltd; 2010;95(11):2126–46. Available from: <http://dx.doi.org/10.1016/j.polymdegradstab.2010.06.007>
88. Okamoto M, John B. Synthetic biopolymer nanocomposites for tissue engineering scaffolds. *Prog Polym Sci* [Internet]. Elsevier Ltd; 2013;38(10–11):1487–503. Available from: <http://dx.doi.org/10.1016/j.progpolymsci.2013.06.001>
89. PINS GD, TONER M, MORGAN JR. Microfabrication of an analog of the basal lamina: biocompatible membranes with complex topographies. *FASEB J* [Internet]. 2000;14(3):593–602. Available from: <http://www.fasebj.org/doi/10.1096/fasebj.14.3.593>
90. Nelson CM, Tien J. Microstructured extracellular matrices in tissue engineering and

- development. *Curr Opin Biotechnol.* 2006;17(5):518–23.
91. Badylak SF, Freytes DO, Gilbert TW. Reprint of: Extracellular matrix as a biological scaffold material: Structure and function. *Acta Biomater* [Internet]. Acta Materialia Inc.; 2015;23(S):S17–26. Available from: <http://dx.doi.org/10.1016/j.actbio.2008.09.013>
  92. Zacchi V, Soranzo C, Cortivo R, Radice M, Brun P, Abatangelo G. In vitro engineering of human skin-like tissue. *J Biomed Mater Res.* 1998;40(2):187–94.
  93. Sun T, Jackson S, Haycock JW, MacNeil S. Culture of skin cells in 3D rather than 2D improves their ability to survive exposure to cytotoxic agents. *J Biotechnol.* 2006;122(3):372–81.
  94. Bonnier F, Keating ME, Wróbel TP, Majzner K, Baranska M, Garcia-Munoz A, et al. Cell viability assessment using the Alamar blue assay: A comparison of 2D and 3D cell culture models. *Toxicol Vitro* [Internet]. Elsevier Ltd; 2015;29(1):124–31. Available from: <http://dx.doi.org/10.1016/j.tiv.2014.09.014>
  95. Onder TT, Gupta PB, Mani SA, Yang J, Lander ES, Weinberg RA. Loss of E-cadherin promotes metastasis via multiple downstream transcriptional pathways. *Cancer Res.* 2008;68(10):3645–54.
  96. Hansen JM, Coleman RL, Sood AK. Targeting the tumour microenvironment in ovarian cancer. *Eur J Cancer* [Internet]. Elsevier Ltd; 2016;56:131–43. Available from: <http://dx.doi.org/10.1016/j.ejca.2015.12.016>
  97. Adams J. The proteasome: Structure, function, and role in the cell. *Cancer Treat Rev.* 2003;29(SUPPL. 1):3–9.
  98. Chitcholtan K, Asselin E, Parent S, Sykes PH, Evans JJ. Differences in growth properties of endometrial cancer in three dimensional (3D) culture and 2D cell monolayer. *Exp Cell*

- Res [Internet]. Elsevier; 2013;319(1):75–87. Available from: <http://dx.doi.org/10.1016/j.yexcr.2012.09.012>
99. dos Santos P, Zanetti JS, Ribeiro-Silva A, Beltrão EI. Beta 1 integrin predicts survival in breast cancer: a clinicopathological and immunohistochemical study. *Diagn Pathol* [Internet]. 2012;7(1):104. Available from: <http://diagnosticpathology.biomedcentral.com/articles/10.1186/1746-1596-7-104>
100. Blackwell KL, Burstein HJ, Storniolo AM, Rugo HS, Sledge G, Aktan G, et al. Overall survival benefit with lapatinib in combination with trastuzumab for patients with human epidermal growth factor receptor 2-positive metastatic breast cancer: Final results from the EGF104900 study. *J Clin Oncol*. 2012;30(21):2585–92.
101. Harris M. Monoclonal antibodies as therapeutic agents for cancer. *Lancet Oncol*. 2004;5(5):292–302.
102. Di C, Zhao Y. Multiple drug resistance due to resistance to stem cells and stem cell treatment progress in cancer (Review). *Exp Ther Med*. 2015;9(2):289–93.
103. Kong B. Tumor initiating cells in pancreatic cancer: A critical view. *World J Stem Cells* [Internet]. 2009;1(1):8. Available from: <http://www.wjgnet.com/1948-0210/full/v1/i1/8.htm>
104. Ozasa H, Oguri T, Uemura T, Miyazaki M, Maeno K, Sato S, et al. Significance of thymidylate synthase for resistance to pemetrexed in lung cancer. *Cancer Sci*. 2010;101(1):161–6.
105. Jiao S, Wang H, Shi Z, Dong A, Zhang W, Song X, et al. A Peptide Mimicking VGLL4 Function Acts as a YAP Antagonist Therapy against Gastric Cancer. *Cancer Cell* [Internet]. Elsevier Inc.; 2014;25(2):166–80. Available from:

<http://dx.doi.org/10.1016/j.ccr.2014.01.010>

106. Calvo F, Ege N, Grande-Garcia A, Hooper S, Jenkins RP, Chaudhry SI, et al. Mechanotransduction and YAP-dependent matrix remodelling is required for the generation and maintenance of cancer-associated fibroblasts. *Nat Cell Biol* [Internet]. Nature Publishing Group; 2013;15(6):637–46. Available from: <http://dx.doi.org/10.1038/ncb2756>
107. Zhao B, Zhao B, Wei X, Wei X, Li W, Li W, et al. Inactivation of YAP oncoprotein by the Hippo pathway is involved in cell contact inhibition and tissue growth control. *Genes Dev*. 2007;21(21):2747–61.
108. Tumaneng K, Schlegelmilch K, Russell RC, Yimlamai D, Basnet H, Mahadevan N, et al. YAP mediates crosstalk between the Hippo and PI(3)K-TOR pathways by suppressing PTEN via miR-29. *Nat Cell Biol* [Internet]. Nature Publishing Group; 2012;14(12):1322–9. Available from: <http://dx.doi.org/10.1038/ncb2615>